



Preliminary Gravity and Ground Magnetic Data in the Arbuckle Uplift near Sulphur, Oklahoma

By Daniel S. Scheirer and Essam Aboud

Any use of trade, firm, or product names is for descriptive purposes only and does not imply endorsement by the U.S. Government

Open-File Report 2008-1003

**U.S. Department of the Interior
U.S. Geological Survey**

This page intentionally left blank

Contents

Abstract	1
Introduction	1
GPS Data	2
Gravity Data	3
Magnetic Data	6
Rock Samples	9
Future Work.....	10
Acknowledgments	10
References Cited.....	13
Appendix: Gravity base stations established by the U.S. Geological Survey near Sulphur, Oklahoma.....	32

Figures

Figure 1. 1a) Topographic map of the Arbuckle Uplift.	14
Figure 1. 1b) Bedrock geology and faults of the Arbuckle Uplift	15
Figure 2. Map of gravity stations.....	16
Figure 3. Difference between gravity station elevations.....	17
Figure 4. Scintrex CG-5 gravity meter.	18
Figure 5. Drift curve for Scintrex CG-5 gravity meter	19
Figure 6a. Isostatic gravity map of Hunton Anticline region	20
Figure 6b. Isostatic gravity map of Chickasaw National Recreation Area	21
Figure 7. Map of magnetic lines collected in May 2007.....	22
Figure 8. Geometrics G-856 proton precession magnetic base station.	23
Figure 9a. Total field variation at the magnetic base station	24
Figure 9b. Total field variation, corrected	25
Figure 10. Geometrics G-858 cesium magnetometer backpack system	26
Figure 11. Magnetic field variability of raw 1-second data	27
Figure 12. Panels illustrating the effects of the cascade of time-series filters	28
Figure 13. a) Magnetic anomalies of the 8 south-to-north profiles.....	29
Figure 13. (ctd.) b) Magnetic anomalies of the 6 west-to-east magnetic profiles.....	30
Figure 13. (ctd.) c) Magnetic anomalies of the west-to-east profile along the seismic line	31

Tables

Table 1. Gravity base stations used for data collected in 2004, 2005, and 2007.....	11
Table 2. Comparison of Scintrex CG-5 and LaCoste-Romberg G8N observed gravity values	11
Table 3. Physical property measurements of rock samples collected in May 2007	12
Table 4. Physical properties of rock samples grouped by stratigraphic unit.....	12

This page intentionally left blank

Preliminary Gravity and Ground Magnetic Data in the Arbuckle Uplift near Sulphur, Oklahoma

By Daniel S. Scheirer¹ and Essam Aboud²

¹US Geological Survey, 345 Middlefield Road, Menlo Park, California, USA

²National Research Institute of Astronomy and Geophysics, 11722 Helwan, Cairo, Egypt

Abstract

Improving knowledge of the geology and geophysics of the Arbuckle Uplift in south-central Oklahoma is a goal of the Framework Geology of Mid-Continent Carbonate Aquifers project sponsored by the United States Geological Survey (USGS) National Cooperative Geologic Mapping Program (NCGMP). In May 2007, we collected ground magnetic and gravity observations in the Hunton Anticline region of the Arbuckle Uplift, near Sulphur, Oklahoma. These observations complement prior gravity data collected for a project sponsored by the National Park Service and helicopter electromagnetic (HEM) and aeromagnetic data collected in March 2007 for the NCGMP project. This report describes the instrumentation and processing that was utilized in the May 2007 geophysical fieldwork, and it presents preliminary results as gravity anomaly maps and magnetic anomaly profiles. Digital tables of gravity and magnetic observations are provided as a supplement to this report. Future work will generate interpretive models of these anomalies and will involve joint analysis of these ground geophysical measurements with airborne and other geophysical and geological observations, with the goal of understanding the geological structures influencing the hydrologic properties of the Arbuckle-Simpson aquifer.

Introduction

The goals of the NCGMP project are to understand the hydrogeology of carbonate aquifers in the mid-continent of North America; the goals of the fiscal year 2007 geophysics task of this project were to characterize the subsurface geological structures that may influence groundwater storage and flow in the Arbuckle-Simpson aquifer, particularly in the Hunton Anticline region of the aquifer system. Proposals to transfer groundwater from this portion of the aquifer have led to numerous studies of the hydrology and geology of the groundwater system (Oklahoma Water Resources Board, 2003). The Arbuckle-Simpson aquifer (Figure 1) is one of the most important bedrock aquifers in Oklahoma (Fairchild and others, 1990). It is comprised of upper Cambrian through middle Ordovician sedimentary units, predominantly carbonates, that are segmented by large- and small-offset faults generated by a series of orogenies in Pennsylvanian time (Ham and others, 1954; Ham, 1969; Johnson, 1990; Hanson and Cates, 1994; Figure 1b). Tectonic deformation culminated in the Arbuckle orogeny, which deposited clastic rocks in much of the area surrounding the outcrop of Arbuckle-Simpson aquifer rocks (Ham, 1969).

The objectives of the geophysical fieldwork conducted in May 2007 were several-fold: to collect ground magnetic and gravity measurements in areas that were surveyed by helicopter in March 2007 as part of the NCGMP task focused on the Arbuckle-Simpson aquifer (Smith and others, in review), to define geophysical signatures of faults where they are exposed as a means of characterizing them where they are buried by younger cover, and to measure the detailed gravity and magnetic fields along a profile coincident with the best (but unpublished) seismic image of basement and supra-basement structures in the Hunton Anticline. The work southeast of Sulphur spans the

area of Block A of the HEM survey, and the work northeast of Sulphur crosses a portion of Block B of the HEM survey (Figure 2; Smith and others, in review).

This geophysical fieldwork builds upon prior investigations funded by the National Park Service to characterize faults in the vicinity of the Chickasaw National Recreation Area (CNRA) using gravity observations (Scheirer and Hosford Scheirer, 2006). The current work focuses to the east and north of the prior project, in areas with sparse gravity observations, and it introduces the ground magnetic method as a complementary tool to characterize the sub-surface.

Gravity and magnetic potential field anomalies reflect changes in the physical properties of rocks at depth. Lateral changes in density and in magnetic susceptibility and remnance of rock units produce gravity and magnetic anomalies, respectively, which then may be used to create qualitative and quantitative models of subsurface geology. Combined with independent constraints from geologic field mapping, borehole analysis, and other geophysical observations, potential field studies provide insight into the buried geological structures and the tectonic development of areas such as the Arbuckle Uplift.

This report documents the global positioning system (GPS), gravity, and magnetic observations made in May 2007, as well physical property measurements of rock samples that were collected. It ends with a description of future work.

GPS Data

Several GPS units with differing precision and accuracy characteristics were used to collect navigation for the geophysical observations. When walking with the magnetic rover system, we used a Trimble Ag-GPS132 system with Omnistar satellite-broadcast differential corrections. This system has a nominal sub-meter horizontal precision, which is excellent for magnetic analysis.

Higher-quality navigation is required for the gravity analysis. Sub-decimeter elevation accuracy is needed to obtain Bouguer gravity anomalies that are more accurate than 20 microgal (μGal , 10^{-8} m/sec^2). Horizontal accuracy is not as crucial as vertical accuracy in the gravity reduction process, although GPS solutions typically provide a horizontal accuracy that is about three times as fine as that of the vertical. Both the accuracy and the precision of a GPS solution are important for evaluating navigation quality, but GPS processing software often reports only precision estimates. Below, we discuss navigation quality using the terms provided by the GPS solution.

We employed two GPS units to measure high-quality locations at gravity stations; both systems utilize dual-frequency carrier-phase antennas and apply differential corrections relative to local base stations after the GPS time-series are recorded. The less precise GPS unit, which measured the positions of all of the gravity stations, was a Trimble GeoXH hand-held unit connected to a dual-frequency Zephyr antenna. Trimble documentation specifies a nominal horizontal RMS accuracy value of 20 cm for the system. The GeoXH station locations are referenced to dual-frequency GPS stations in the vicinity. In this case, we utilized the 5 continuously operating reference stations (CORS) that were within 100 km of Sulphur, Oklahoma: Ada, Ardmore, Duncan, Purcell, and Tecumseh. Using Trimble Pathfinder Office software, the calculated precisions of the gravity stations were somewhat better than the nominal 20-cm accuracy value, with 85% of the values having horizontal precisions better than 15 cm. As noted above, vertical uncertainty is likely to be about three times as great as horizontal uncertainty.

The more precise system, a Trimble R8 rover and base system, was used in a post-processed kinematic (PPK) observation mode. We tested a real-time kinematic (RTK) observation mode in a prior field-session in this area with a Trimble 4700 GPS system but experienced significant times of radio shadowing or out-of-radio-range conditions across the area. The GPS base station was deployed on a stake in the center of the backyard of the Bostick House (1147 W. 1st St., Sulphur, OK) and was named BOSTICK. To establish the precise location of BOSTICK, we collected >5 hour occupations on multiple days and submitted them to the National Geodetic Survey's (NGS) Online Positioning User Service (OPUS), which uses three reference stations in the region to differentially calculate a high-precision location of the base station. We adopted a representative OPUS solution for the BOSTICK position of: Northing 3820547.963 m, Easting 686539.817 m, ellipsoidal height 279.766 m, in UTM

zone 14N with the NAD83 (CORS96) datum. This position has precisions of 17 mm in the N-S direction, 8 mm in E-W, and 12 mm in height.

The base and rover receivers recorded GPS data every 1 second. The Trimble R8 rover data were acquired at gravity stations during 3-minute occupations. Once or more per day, we lost carrier-phase lock on the rover receiver and we had to reacquire it; these instances generally occurred when we passed beneath heavy foliage. At two gravity stations (07S072 on 2007May12 and 07S146 on 2007May16), the PPK GPS solution type was “Iono Free Float”, a lower quality solution than the “Iono Free Fixed” solutions at the other gravity stations, a consequence of poor GPS acquisition conditions. At one additional station, 07S134 (2007May15), the GPS solution had extreme errors (precisions in thousands of kilometers) and this solution blunder was omitted from further analysis.

To test the quality of the BOSTICK location and of the PPK method, we occupied NGS benchmark EL0793 (designated NEAL and stamped “NEAL 1954”), located on the top of a hill a few kilometers southeast of Sulphur on Gene Neal’s ranch. The differences between the PPK solution and the NGS published position for NEAL are: $\Delta N=57$ mm; $\Delta E=6$ mm; $\Delta Z=17$ mm, where Z is ellipsoidal height. The easting and height differences are extremely small, especially since the NGS published height is assigned an uncertainty of ± 20 mm. The 57 mm northing difference is larger than we expected with the PPK technique, and we do not have a good explanation for it.

Trimble documentation for the R8 system indicates uncertainties of 10 mm and 20 mm in horizontal and vertical positioning of the rover in the immediate vicinity of a base station; in addition, there is a 1 ppm increase in horizontal and vertical uncertainties as baseline distance increases. The most distant gravity station, 07S069, was ~ 31 km from BOSTICK, which would suggest a 1 ppm additional uncertainty of 31 mm in both horizontal and vertical (yielding a total uncertainty of ~ 40 mm in horizontal and ~ 50 mm in vertical). Because the 17 mm agreement of the published and PPK ellipsoidal heights of NEAL was both within the ± 20 mm uncertainty of the NGS datasheet value and within the ± 24 mm (20 mm + 4 mm) values suggested by the Trimble documentation, we have confidence that the equipment, the acquisition, and the processing procedures performed well in determining ellipsoidal height. For gravity stations where we had good PPK solutions, the vertical precision is 5 cm or better.

The Trimble R8 system provided elevations for 112 gravity stations, slightly more than two-thirds of the total collected in May 2007. Gravity stations without Trimble R8 solutions occurred at times when the base GPS receiver was not functioning correctly.

A comparison of elevations at the 112 gravity stations that have both Trimble R8 and Trimble GeoXH positions is shown in Figure 3. The average difference (GeoXH – R8 elevation, Figure 3 top panel) is 6 cm, with a standard deviation of 59 cm. Omitting the 4 stations where the difference exceeds 150 cm, the average difference is 4 cm, with a standard deviation of 36 cm. The elevation difference at many gravity stations is greater than what one might expect based on the calculated vertical precisions of the two GPS units’ solutions (Figure 3 bottom panel), indicating that unmodeled biases may be present in the GPS solutions.

For geophysical analysis, GPS elevations recorded as ellipsoidal heights were first converted to orthometric (relative to sea-level) heights using the NGS GEOID03 software, then converted from the NAVD88 height datum to NGVD29 using the NGS VERTCON software. Geographic coordinates were converted from the NAD83 horizontal datum to NAD27 using the NGS NADCON software. For a location in the western-end of Sulphur (97°W , 34.5°N): the longitude shift going from NAD83 to NAD27 is $+27.122$ m and the corresponding latitude shift is $+9.870$ m, using the NADCON software. In other words, the NAD27 longitude and latitude values for points in this area are slightly greater than their corresponding NAD83 values. Using the VERTCON software, the NAVD88 orthometric height is 0.073 m (7.3 cm) higher than the NGVD29. Using the GEOID03 software, the ellipsoidal height is 25.282 m lower than the orthometric height. (Using GEOID99, this difference is 25.257 m.) These datum differences do not change appreciably over the lateral span of the study area. We carefully accounted for these datum shifts as we investigated the accuracy and precision of the GPS locations.

Gravity Data

We collected gravity observations at 166 new sites in the greater Hunton Anticline area southeast and northeast of Sulphur, Oklahoma (Figure 2). We used two gravity meters: a LaCoste-Romberg G-meter, G8N, which has an Aliod electronic nulling upgrade, and a Scintrex CG-5 Autograv system (serial number 070340243). This

was the first field session that utilized the CG-5 gravity meter. Both of the gravity meters compute a gravity reading from a filtered time series of raw readings over a specified interval of time. With the CG-5 meter, we used occupation times of 60 seconds; with the G8N meter, we used occupation times of 40 seconds. Both of these time intervals were recommended by the instrument manufacturers. At each gravity station, we collected between 2-4 occupations; when a subsequent gravity reading was close to its predecessor, generally within 5 μGal , we assigned the latter gravity reading as the value for the station.

We utilized the gravity base station PVENDOME that was established for the 2004 and 2005 gravity fieldwork (Scheirer and Hosford Scheirer, 2006), situated in the parking lot of Vendome Well in CNRA. Table 1 and the base station data sheets in the Appendix provide information about PVENDOME and other gravity base stations used in this area. We visited PVENDOME at the beginning and end of each gravity field day, taking a reading with the gravity meters that were used during that day. Based on May 2007 repeat readings between PVENDOME and the neighboring gravity base VENDOME (Table 1 and Appendix 2), we adjusted the IGSN71 gravity value of PVENDOME downward by 30 μGal (Table 1) relative to that used in Scheirer and Hosford Scheirer (2006).

Gravity observations were made adjacent to the field vehicle (Figure 4) along public roadways, generally along section-line roads. Stations were located both to fill existing gravity coverage gaps and to collect high-resolution profiles along select roadways (Figure 2). Of the high-resolution gravity lines, three ~8-km-long (~5 mile) north-south profiles were collected at 400 m (~1/4 mile) spacing southeast of Sulphur, and one ~19-km-long (~12 mile) east-west profile was collected along the seismic line road northeast of Sulphur. In addition to these detailed profiles, we collected data along other roadways to complement station coverage from the 2004 and 2005 gravity field sessions, and we collected data in previously unoccupied areas at a minimum station spacing of 1.6 km (1 mile). In these latter cases, we often collected stations at the intersections of section line roads (Figure 2).

Because the Scintrex CG-5 meter had never been used in the field before, we collected measurements with both gravity meters on 2007May09. By keeping track of station-to-station changes in gravity readings as we collected them, we determined that the instruments agreed to better than 0.05 mGal (50 μGal), for 12 stations over a time-span of 4 hours. In addition, we collected one station with both gravity meters on 2007May11. The difference between the computed observed gravity values measured by both meters at these 13 sites, after accounting for tides, instrument drift, and calibration factors, ranged between -48 and +1 μGal (Table 2). The average difference was -14 μGal , with a standard deviation of 13 μGal . This average is influenced by two relatively large differences at the end of 2007May09 (Table 2); the range of the other 11 differences is -17 to +1 μGal , and their average is -9 μGal , with a standard deviation of 6 μGal .

In processing the gravity data, we corrected for instrument drift in both meters by considering the difference between the tide-corrected gravity readings at the gravity base station at the beginning and end of each day. At the end of each field day, we calculated this difference, or closure, to assess the behavior of the meters. The gravity base differences for the LaCoste-Romberg G8N meter were +18, -34, +22, and -20 μGal for the 4 days when we collected new stations with this meter (May 08, 09, 11, and 14); these closure values are typical for this type of meter. The differences between the LaCoste-Romberg and Scintrex CG-5 readings on 2007May09 and 2007May11, noted above, are generally smaller than the LaCoste-Romberg daily drifts.

The base closure values for the Scintrex CG-5 were much greater (pink lines in Figure 5), a result of inadvertently setting the time-zone incorrectly in the meter, which yielded improper tide corrections. After recognizing and correcting this error, we consistently measured field-day drifts of +20 to +40 μGal (black lines in Figure 5), with greater differences toward the end of the field session. After omitting a faulty CG-5 base reading at the beginning of May 14, a multiday drift curve was established (orange line in Figure 5) and applied to all of the CG-5 readings. For the time-span of the fieldwork, the average drift was 86 $\mu\text{Gal}/\text{day}$, which is typical for quartz-spring meters such as the CG-5 and is significantly larger than the drift of metallic-spring meters such as the LaCoste-Romberg G-meter. That said, quartz-spring meters have stable drifts, which justifies using a piece-wise linear drift curve (Figure 5).

As a test of the repeatability of the CG-5 gravity values, we measured PVENDOME at an intermediate time between the start- and end-of-day readings on 2007May11. Using the drift defined by those readings, the observed gravity value of the intermediate PVENDOME occupation was calculated to be 1 μGal greater than the prescribed value. In addition, on 2007May12 we reoccupied four CG-5 gravity stations that had been collected on 2007May11 because we feared that there had been an instrument tare in that prior day's measurements (pink line of Figure 5, before we recognized the time-zone error in the real-time tide corrections). The observed gravity values of these

four stations differed by -10, +3, +12, and +24 μGal (later minus earlier occupation values). Our ability to collocate these repeat readings was limited by a real-time GPS unit's accuracy of only several meters; thus some of the gravity differences at these four stations may reflect small changes in elevation between the former and latter occupation stations.

We processed the observed gravity measurements using a standard sequence of anomaly reductions (e.g. Blakely, 1995), including global, free-air, Bouguer, terrain, curvature, and isostatic effects. The final gravity anomaly after incorporating these effects is termed the isostatic gravity anomaly, and it is useful for interpretation because it primarily reflects the density variations in the upper- and mid-crust (Simpson and others, 1986). The two greatest sources of uncertainty in this reduction sequence are determining the elevation of the gravity station and estimating the value of the terrain correction. An uncertainty of 1 meter in station elevation translates into an uncertainty in free-air anomaly of ~ 0.3 mGal (300 μGal); that same elevation uncertainty translates into Bouguer uncertainty of ~ 0.2 mGal (200 μGal). As described above, we endeavored to obtain sub-decimeter elevations at gravity stations, with the goal of reducing Bouguer and isostatic anomaly uncertainties to 20 μGal or smaller.

We estimated terrain corrections from the site of the gravity station to a radius of 68 m (223 feet, the outer radius of the Hayford B zone) using graphed curves of local terrain corrections. We located our gravity stations as far away from topographic variation as possible to minimize these innermost, or field, terrain effects. Field terrain corrections were assigned a nominal value of 10 μGal , except at a few stations where field terrain corrections were estimated to be larger, with a maximum of 30 μGal .

Terrain corrections at greater distances were calculated from 10 m digital elevation models (DEMs) in two stages: from 68 m to 2 km and from 2 km to 167 km using the algorithm of Plouff (1977). In the 2007 campaign, the greatest total terrain correction was just under 300 μGal , and 90% of the corrections were between 50 and 200 μGal . A rule-of-thumb for terrain corrections is that their uncertainty is often $\sim 10\%$ of their total value, suggesting that the uncertainties in terrain correction were typically 5-20 μGal , and as much as 30 μGal .

The observed gravity and field terrain correction values for stations collected in May 2007 were combined with those collected in 2004 and 2005 (Scheirer and Hosford Scheirer, 2006) and with observed gravity values from Cates (1989) and from the GeoNet database (Hildenbrand and others, 2002). Because of the adjustment to the gravity base value at PVENDOME, noted above, we recalculated the observed gravity values at approximately two-thirds of the stations collected in 2005 (GEM102-GEM327). In addition, we identified a 0.4 mGal tare in gravity data collected on 2005May09, and we adjusted the observed gravity values of 11 stations (GEM308-GEM318) to account for that tare. Based on comparisons of gravity values at neighboring stations, we adjusted the Cates (1989) gravity values by -28.1 mGal and the GeoNet gravity values by +0.8 mGal; these adjustments made the prior gravity values consistent with the 2004, 2005, and 2007 values.

For the Cates (1989) and GeoNet stations, the innermost terrain corrections were not available. The location and gravity precision of these two data sets was not as high as data collected in 2004, 2005, and 2007. Geographic locations were provided with a precision of 30 m (1 arc second) in the Cates (1989) data table, and station elevations were interpolated from topographic maps having 10-foot contours. For the GeoNet stations, the geographic precision of the geographic coordinate values is ~ 10 m, and the source and uncertainty of the elevation values are not provided. Gravity values were provided to the nearest 100 μGal for the Cates (1989) stations and to the nearest 10 μGal for most of the GeoNet stations.

To test the validity of the gravity station locations, we compared the tabulated elevations of the ~ 800 stations in the study area with elevations interpolated from 10 m DEMs. For the GeoNet data, 10% of the stations had elevations that differed by >10 m from the DEM elevations, and these stations were omitted from analysis. Otherwise, all of the tabulated elevations were within 10 m of their DEM counterparts. For gravity stations collected in 2004, 2005, and 2007, virtually all had elevations within 1 to 3 m of the DEM elevations, confirming the high quality of the differential GPS solutions. Also, because of the heterogeneous and uncertain origin of the GeoNet gravity observations (collected with multiple gravity meters, observers, base stations, and goals), we excluded GeoNet stations located close to gravity stations collected as part of studies of the Arbuckle-Simpson aquifer (Cates, 1989; Scheirer and Hosford Scheirer, 2006; May 2007 fieldwork): 22 of the 97 GeoNet stations within the study area were omitted because they were located within 500 m of stations from these local surveys.

The parameters used in the calculation of gravity effects are typical for continental gravity studies; these include an upper crustal density of 2.67 g/cm³, a mantle-crust density contrast of 0.4 g/cm³, and a nominal crustal thickness at sea level of 40 km (Braile, 1989). A typical uncertainty of a gravity anomaly from a May 2007 gravity

station is estimated to be ~ 50 μGal ; uncertainties from the 2004 and 2005 gravity stations, with slightly poorer elevation control, were estimated to be ~ 150 - 200 μGal , and uncertainties of Cates (1989) and GeoNet stations are more variable and likely to be larger, due to greater uncertainties in station elevation.

A digital table of principal facts for all of the gravity stations used in this study is provided as a supplement to this report.

Isostatic gravity station data were gridded with 200 m spacing, which is finer than the average station-spacing of ~ 1500 m, determined from a triangulated network of the stations in Figure 2; for the dense station coverage between the towns of Sulphur and Mill Creek, the average station spacing is 700 m. We investigated whether any of the stations had gravity values significantly different from their neighbors by upward-continuing (for example, Blakely, 1995) the isostatic gravity field by 200 to 500 m, then calculating the difference between the original and upward-continued grids. Large differences highlight short-wavelength anomalies in the grid that are likely related to poor gravity data. In this way we determined that only two noisy stations, Cates001 and Cates119, were present, and these were omitted from the final isostatic gravity grid. This noise identification technique is effective only where a gravity station with a bad value is close, within a handful of grid-cell distances, to other stations with good values.

Overviews of the gravity data are presented as contour maps of the isostatic anomaly in Figures 6a and 6b. The pattern of gravity anomalies reflects significant density contrasts across the major faults in the study area. The most positive gravity anomalies occur where Precambrian basement crops out or is shallow (Figure 1b), south of the Reagan Fault (RF in Figure 6) in the Tishomingo Anticline. The Mill Creek Syncline, between the Reagan and Mill Creek Faults (RF and MCF in Figure 6), is a relative gravity low, with an oval minimum near its western end. The Belton Anticline, between the Mill Creek and South Sulphur Faults (MCF and SSF in Figure 6), is a relative gravity high, and the Sulphur Syncline between the South Sulphur and the Sulphur Faults (SSF and SF in Figure 6) is a smaller-amplitude low. North of the Sulphur Fault, the Hunton Anticline is associated with a smooth gravity gradient that decreases to the north. None of the minor faults (dashed lines in Figure 6) has a clear signature in the isostatic gravity field. The alternating pattern of gravity highs and lows corresponds with structural highs and lows, indicating that the top of high-density basement is a significant control on the gravity anomaly in this area of the Arbuckle Uplift.

Magnetic Data

We collected magnetic traverses with a backpack system walking along roadways in the study area (Figure 7). The total length of these traverses was 110 km (70 miles), spanning slightly more than 22 hours of walking. The traverses form a loose network of fourteen 4- to 12-km-long lines southeast of Sulphur, plus an isolated 19-km-long traverse northeast of Sulphur along a roadway where a seismic reflection line was collected in 1979. These rover magnetic observations were referenced to magnetic base station observations (Figures 8 and 9) to remove diurnal magnetic field variations that occurred during the walking surveys.

A summary of the magnetic base station data is shown in Figure 9a. The magnetic base station was a Geometrics G-856 proton precession magnetometer, configured to collect total field data every 5 seconds. Typical of proton precession data, the raw observations contained short-period scatter of ~ 5 nanotesla (nT), which was filtered to recover the smooth variations expected for the natural field at the magnetic base. We applied a median filter (1-minute-wide) to despiked the observations, and then ran them through a Gaussian filter with a 5-minute-wide standard deviation to achieve smooth variations (Figure 9a, lower panel). Other simple filters with similar widths produce near-identical output.

On the first magnetic survey day (2007May08), the magnetic base was located near the BOSTICK GPS base station. This site was within 10 m of driveways, and the arrival and departure of vehicles in those driveways produced anomalies 10-50 nT in magnitude (red triangles in Figure 9a, lower panel), which are large compared to the ~ 40 nT diurnal variation of this area. On subsequent days, we located the magnetic base at a magnetically quiet site in CNRA, ~ 150 m east of Vendome Well along the north bank of Rock Creek and hidden from the view of park pathways. The location of this magnetic base is $34^{\circ}30.31'N$, $96^{\circ}58.28'W$ (NAD27), with an elevation of 290 m (953 feet). The current International Geomagnetic Reference Field model, IGRF2005, parameters for this site in May 2007 are: total field, $F=51017$ nT; inclination, $I=+63.4^{\circ}$ (down); declination, $D=+4.6^{\circ}$ (east of North).

Magnetic base data from 2007May09 to 2007May15 show a consistent diurnal fluctuation characterized by a 30-40 nT trough centered at ~1130 Central Daylight Time (CDT) followed by a smaller peak at ~1700 CDT (Figure 9a).

The top panel of Figure 9a shows the measured total field at the CNRA magnetic base compared to adjusted total field measurements at the two closest magnetic observatory sites, BOU (Boulder, CO) and BSL (Bay St. Louis, MS). These observatory field values have been adjusted in two ways: a time-shift has been applied to account for the longitude difference between the CNRA base and the observatories, and the total field values have been shifted to make them agree with the total field at CNRA. The former adjustment is appropriate for diurnal fluctuations with gradual spatial variations, and the latter adjustment accounts for the different magnetic latitudes of these three sites. A number of observations can be made about the base magnetic data from the top panel of Figure 9a. First, the magnetic surveys were conducted during a time without magnetic storms, which would have produced non-periodic variations an order of magnitude greater than observed. Second, the quiet night-time total field value of the CNRA base is 15-20 nT lower than the IGRF2005 predicted value, a difference that is not remarkable given both the uncertainties in the IGRF2005 predictions and the magnetic anomalies typical of geological sources in this area. Third, the CNRA base station curves for 2007May09 and 2007May11 appear to be ~20 nT greater than the curves for the other days. We do not have an explanation for this difference: the magnetic base was sited far away from observable magnetic objects and the base sensor was placed in as consistent a location as possible from day-to-day. Nonetheless, we reduced the CNRA base station total field values on those two days to make them consistent with other values (Figure 9b) for subsequent analysis. In addition, we applied ad-hoc step corrections to the magnetic base record of 2007May08 at five times when it was influenced by near-by vehicles (Figure 9b, red triangles). These corrected CNRA base magnetic values (Figure 9b) were subtracted from magnetic rover measurements to account for diurnal magnetic total field fluctuations.

Magnetic rover data were collected with a Geometrics G-858 cesium magnetometer sampling every 1 second. The total field magnetometer was mounted in a backpack system (Figure 10), and the magnetic sensor at the top of the pole was ~2.5 m above the ground. Rover data were collected while walking at typical speeds of 5 km/hour (3 miles/hour), which yields an along-profile spacing of observations slightly less than 1.5 m. Navigation was collected using a non-magnetic Trimble Ag-GPS132 system (Figure 10) that utilizes differential GPS corrections broadcast from a satellite, with a specified horizontal precision of <1 m.

At ground-level in built-up areas, magnetic fields from anthropogenic sources usually overwhelm the fields from geological sources. The anthropogenic fields in the study area arise from buried pipes, bridges, power-lines, vehicles, quarries, and metal fences and gates (Figures 10 and 11). These fields have anomalies typically in the range of 100-2,000 nT; the fields arising from geological sources in the study area have anomalies typically 10-100 nT. A major effort of processing the ground magnetic survey data was separating man-made from natural fields. As we collected the rover magnetic data, we noted times when we passed magnetic objects to characterize their anomalies in the data (Figure 11). In addition, we walked along the roadways in a manner to minimize man-made anomalies; we shifted from side-to-side of a road to increase our separation from metallic gates or power-lines that paralleled the road, and we stopped walking when we were approached and passed by vehicles.

During the first magnetic survey day (2007May08), we attached 2 magnetometer sensors to the survey pole as a means of calculating vertical gradients in the magnetic total field over the sensor separation distance of 66 cm (Figure 10). The Geometrics G-858 manual recommends this mode of measuring vertical gradiometry to identify and characterize magnetic sources that are located within about 5-separation-distances of the sensors. In our experiment the sensor separation corresponds to a distance of ~3 m, which is poor for detecting buried objects because it is not much greater than the average height (~2.2 m) of sensors above the ground (Figure 10). Nonetheless, we tested this gradiometry mode as a means of detecting shallow man-made magnetic sources that might otherwise be obscured. The results of this test were several-fold: all close magnetic objects produced different fields at the upper and lower sensors (hence, significantly non-zero vertical gradients), the lower sensor became saturated and produced “drop-out” readings much more frequently than the upper sensor, and all non-zero vertical magnetic gradients were associated with large total field anomalies in both sensors. This latter observation indicated that the two-sensor approach did not provide additional useful information in this setting. The battery-life of the dual-magnetic-sensor+GPS system was ~40% shorter than that of the single-magnetic-sensor+GPS system, so we conserved power and reduced backpack weight by continuing with only one sensor. We placed this sensor at the top of the survey pole (Figure 10) to separate it from man-made sources as much as possible.

The magnetic traverses southeast of Sulphur (Figure 7) follow virtually all publicly accessible roadways in the Block A survey area of the HEM experiment (Smith and others, in review). It would be possible to collect

additional data within the boundaries of private ranches with permission, but the rate of progress would be much slower and the traverses more curved. The magnetic traverse northeast of Sulphur (Figure 7), along the section line road where the OK-3-80 seismic line was shot in 1979, crosses the Block B survey area of the HEM experiment. Several roadways extend to the north of this magnetic traverse, but no roadways extend to the south. Again, permission might be obtained to collect cross-line data.

Published aeromagnetic observations in south-central Oklahoma are low-resolution and were collected as part of the National Uranium Resource Evaluation (NURE) program (Sweeney and Hill, 2005). The survey that spans the Arbuckle Uplift was conducted in August and September of 1976 with ~5-km-spaced (3-mile) flight lines oriented in an east-west direction at a nominal altitude of 120 m (400 feet) above-ground. The magnetic data collected in conjunction with the HEM survey in March 2007 over four survey areas of the Hunton Anticline region (Figure 2, brown lines) are superior to the NURE observations in a number of ways: they were flown with line spacings of 800 m and 400 m ($\frac{1}{2}$ and $\frac{1}{4}$ -mile), at a nominal drape altitude of 30 m (100 feet), and perpendicular to the major geologic structures.

Processing the magnetic rover data was accomplished in a number of steps. Segments of the raw magnetic time-series were selected and joined together, where needed, to form the 15 survey lines. Then, the magnetic values were filtered in the time-domain with a series of robust filters (Figure 12) to remove most of the anthropogenic anomalies. Diurnal variation was removed from the filtered time-series. Finally, the magnetic values were binned to a constant-spacing of 25 m along each profile, and the IGRF2005 values were removed from each binned total field value. The IGRF total field increases by 135 nT from the southern to northern limits of the study area, and it increases by 21 nT from west to east. Along the longest north-south line, the IGRF value varies by 50 nT; along the longest east-west survey line (the seismic line road), the IGRF value varies by 12 nT.

The series of time-domain filters (Figure 12) was applied as a cascade; it was designed not simply to smooth the magnetic data but rather to reject values arising from anthropogenic sources. First, magnetic values greater than 1000 nT from an average IGRF2005 value (51,000 nT) for the study area were voided; this rejected ~1% of the values, including magnetic drop-outs and the largest anomalies from man-made sources. Second, magnetic values were voided from times when we were slowing, stopped, or resuming speed, such as when we were being passed by vehicles or exchanging walkers (Figure 12a, ~2% additional rejected). Third, values were voided that differed by 300 nT from the median value of those in 10-min-wide windows centered on the value in question (Figure 12b, ~2.5% additional rejected). Fourth, values were voided that differed by 100 nT from the median value of those in 10-min-wide windows centered on the value in question (Figure 12c, ~7% additional rejected). Fifth, values were voided that differed by 25 nT from the median value of those in 2-min-wide windows centered on the value in question (Figure 12d, ~14% additional rejected). Sixth, we omitted values close to (within 5-seconds of) values voided in the prior steps. In sum, about 26% of the raw observations were voided as a result of these filters, signifying the preponderance of anthropogenic fields in this area.

For the example illustrated in Figure 12, natural field variability of 300 nT is superimposed with dozens of short-wavelength, >100 nT anthropogenic anomalies. Figure 11 illustrates the effects of the time-series filter cascade on a section of data when we passed noise sources that we noted. We tested other robust filter schemes that resulted in a similar culling of the raw data. Any non-robust smoothing filters, such as moving averages or other convolutions, will perform poorly with raw magnetic values that have poor signal to noise characteristics such as this ground magnetic data set. The sequence of median filters, using larger to smaller reject-thresholds, is necessary because numerous time-spans have >50% anthropogenic noise, and the approach of sequentially removing the most extreme values promotes the retention of noise-free values in the final output.

The magnetic profiles are illustrated in Figure 13, separated into south-to-north lines, west-to-east lines in the main study area, and the west-to-east line along the seismic reflection profile (Figures 13a, 13b, and 13c, respectively). The difference in scatter between the light-gray and blue curves indicates the effect of the anthropogenic source filter, described above, and the anomaly offset between them (most easily seen at greater distances in Figure 13c) shows the diurnal correction. The noise level of the magnetic lines varies considerably, and is especially great for the north-south oriented lines such as lines 04 and 14, which followed narrow roadways where power lines were close to the roads. All of the filtered anomalies (blue lines in Figure 13) have a short-wavelength scatter of 5-10 nT. The 20-30 m wavelength of this scatter indicates that it originates from sources within tens of meters of the magnetic sensor, but its persistence and its wavelength and amplitude characteristics do not permit removal with the robust filter cascade. To model magnetic sources from hundreds of meters to kilometers in depth, one should model only the longer-wavelength components of these profiles. One could smooth these data (for

example, Figure 13c, where green lines show Gaussian function convolutions) or fit smooth functions to the observations to obtain profiles less influenced by proximal magnetic sources.

Profiles derived from the 1-km-spaced aeromagnetic grid of Oklahoma (Sweeney and Hill, 2005; purple lines in Figure 13) are superimposed beneath the ground magnetic variation. Where the ground magnetic profiles vary smoothly, for example along the west-to-east profiles of Figure 13b, the ground magnetic anomalies agree closely with the aeromagnetic gridded values. For the south-to-north lines, the agreement is poorer, especially where ground magnetic gradients are large (lines 14 and 04). Several factors account for this disagreement. The original NURE flight-line data were acquired at 120 m (400 feet) above-ground, and the data were upward-continued to 300 m (1000 feet) before gridding, thus limiting the maximum gradient of the gridded magnetic data. Second, the NURE flight-lines were primarily oriented east-west at a spacing of ~5 km (3 miles), so north-south profiles extracted from these grids are likely to be highly influenced by the gridding algorithm and the particular locations of the flight-lines. For the west-to-east magnetic line 08 (Figure 13c), the gridded aeromagnetic profile contains spectral content similar to the 800-1600 m Gaussian filtered ground magnetic anomaly, consistent with the 300 m upward continuation applied to the NURE flight-line data.

The largest magnetic anomaly that can be attributed to geological structure is at the Reagan Fault crossed by lines 14 and 04 (Figure 13a), where Precambrian basement outcrop to the south is juxtaposed against Paleozoic carbonate units to the north (Figure 1b). The amplitude of this anomaly is ~1000 nT. To the west of lines 14 and 04 where basement rocks south of the Reagan Fault are buried, the magnetic anomaly associated with the Reagan Fault is much smaller (lines 07 and 01, Figure 13a). More subtle anomalies, on the order of 50-200 nT are observed in all of the other lines, and they correlate from line to line (Figure 13a, b). The Mill Creek Fault trace is consistently located near the top of an increasing-to-the-north magnetic gradient. The South Sulphur Fault and the Sulphur Fault do not correspond to significant magnetic anomalies.

A digital table of the ground magnetic data is provided as a supplement to this report.

Rock Samples

We collected 11 hand-samples at gravity stations located adjacent to rock outcrops. We measured the sample density (Johnson and Olhoeft, 1984) and magnetic susceptibility properties in the lab (Table 3). The physical property values of the Paleozoic carbonate and Precambrian basement rock samples were added to the compilation of Scheirer and Hosford Scheirer (2006). While these measured physical properties may differ from the bulk, in situ properties that generate the observed gravity and magnetic anomalies, they can be used to guide the selection of density and susceptibility values in forward models of the observed anomalies.

Rock property measurements from this study and from Scheirer and Hosford Scheirer (2006) are grouped by stratigraphy in Table 4. The most common rock sampled is carbonate from the lower Paleozoic Arbuckle Group, largely of dolomitic composition, with a saturated bulk density similar to the 2.67 g/cm³ assumed for the Bouguer and isostatic gravity calculations. The clastic Paleozoic rocks generally have densities 0.1 to 0.2 g/cm³ lower than the 2.67 g/cm³ Bouguer reduction density. The youngest, Pennsylvanian age rocks sampled, arkosic and conglomeratic units of the Vanoss Group, generally have even lower densities. The densities of Precambrian basement samples average to the Bouguer reduction density, and two of the Precambrian basement samples have the highest densities measured in the sample suite. As discussed above, the pattern of gravity anomalies indicates that the in situ density of the basement rocks is on-average significantly greater than the density of the overlying carbonate and clastic units, even though hand sample density measurements of the basement rocks are not statistically different from those of the Arbuckle Group samples (Table 4).

In terms of magnetic properties, the basement rock samples are the only ones that have significantly non-zero magnetic susceptibilities (Tables 3 and 4), although it is not yet determined if small differences in susceptibility (of order 10⁻⁵ SI) of the Paleozoic units might produce observable magnetic anomalies at ground or low-elevation HEM survey levels.

Future Work

Future investigations of the gravity data set will involve several approaches. By identifying gradients in the gridded isostatic gravity field, we will detect and characterize significant lateral density interfaces in the subsurface (Blakely and Simpson, 1986). Depth-to-source techniques applied to gravity anomaly grids and profiles will provide estimates to the depth of the dense basement interface, which is critical to understand the depth limits of the Arbuckle-Simpson aquifer. In addition, we will conduct forward modeling (for example, Talwani and others, 1959) of the high-resolution gravity profiles, incorporating mapped geological units and faults and incorporating constraints from ground magnetic and aerogeophysical anomalies. The expanded lateral gravity coverage and the improved resolution along a number of north-south profiles will allow improved interpretations relative to those presented in Scheirer and Hosford Scheirer (2006).

Future work with the magnetic profiles will develop forward models of geologic structures that can generate both these magnetic anomalies and coincident high-resolution gravity anomalies. Where the ground magnetic data coincide with the HEM aeromagnetic survey data (Figure 7), we can compare the shape and amplitude of magnetic anomalies at ground and ~30 m above-ground levels. Differences in these anomalies provide a vertical gradient measure. Using the rule-of-thumb, noted above, relating sensitivity distance to a maximum of about five times the observation level separation distance, these magnetic anomaly differences will be most sensitive to structures in the uppermost ~150 m of the subsurface. This depth is similar to the maximum depth of resistivity information afforded by the HEM observations (Smith and others, in review).

Acknowledgments

We thank the USGS National Cooperative Geologic Mapping Program for supporting this work. We are grateful to the Egyptian Government for providing funds for Essam Aboud to work with the Menlo Park geophysics group, GUMP, during half of 2007. We thank the USGS Water Resources Discipline office in Oklahoma City for providing a differential GPS system and a field vehicle for our use. Marvin Abbott and Scott Christenson, now in the Albuquerque Office, prepared the Trimble R8 GPS equipment and developed an acquisition protocol for the PPK mode that we required. Stan Paxton facilitated the use of the field vehicle. We are grateful to Noel Osborn and the Oklahoma Water Resources Board for providing Joseph Zume and Carlos Uribe as field assistants during about half of our field-days. We thank Joseph and Carlos for their enthusiastic help and companionship, and for sharing their knowledge of the Hunton Anticline. We thank Allegra Hosford Scheirer for providing field support. We thank Darryl Carter for sharing knowledge about the field area, we thank Gene Neal for access to a NGS benchmark on his ranch, and we thank Steve Burrough of the CNRA for granting permission to site our magnetic base station in the Park. This report was improved by reviews of Philip Brown and Victoria Langenheim.

Table 1. Gravity base stations used for data collected in 2004, 2005, and 2007

[Datums: gravity, IGSN71; (27), NAD27 horizontal datum; (83), NAD83 horizontal datum; (29), NGVD29 vertical datum; (88), NAVD88 vertical datum. The only significant difference of this table from Table 3 of Scheirer and Hosford Scheirer (2006) is a 0.03 mGal reduction in the PVENDOME observed gravity value, below.]

Base name	Latitude N	Longitude W	Elevation (m)	Observed gravity (mGal)	Description
COALGATE ¹	34° 32.23' 34° 32.24'	96° 13.11' (27) 96° 13.13' (83)	185.9 (29) 186.0 (88)	979,626.22	Coalgate, Okla. Fire Station (codes ACIC 3841-2; IGB 11846B)
VENDOME	34° 30.348' 34° 30.353'	96° 58.378' (27) 96° 58.396' (83)	288.4 (29) 288.5 (88)	979,648.02	Vendome Well, CNRA, Okla.
PVENDOME	34° 30.346' 34° 30.351'	96° 58.353' (27) 96° 58.371' (83)	287.8 (29) 287.9 (88)	979,648.08	West End of Parking Lot of Vendome Well, CNRA, Okla.
RCC12	34° 29.865' 34° 29.870'	96° 59.211' (27) 96° 59.229' (83)	284.3 (29) 284.4 (88)	979,647.26	Rock Creek Campground, Site 12, CNRA, Okla.

¹Part of the World Relative Gravity Reference Network (Jablonski, 1974).

Table 2. Comparison of Scintrex CG-5 and LaCoste-Romberg G8N observed gravity values

[Base station drift (end-of-day minus start-of-day readings) of LaCoste-Romberg meter G8N on 2007May09 was -34 μ Gal; on 2007May11 it was +22 μ Gal.]

Gravity station name	CG-5 reading date/time (local, CDT)	Observed gravity difference ¹ (μ Gal)
07s009	2007May09/14:40	-2
07s010	2007May09/15:00	-15
07s011	2007May09/16:07	-12
07s012	2007May09/16:26	0
07s013	2007May09/16:41	-13
07s014	2007May09/16:58	-6
07s015	2007May09/17:18	-17
07s016	2007May09/17:29	-8
07s017	2007May09/17:51	-12
07s018	2007May09/18:08	1
07s019	2007May09/18:24	-48
07s020	2007May09/18:37	-29
07s054	2007May11/13:26	-15

¹Observed gravity difference computed by subtracting LaCoste-Romberg observed gravity value from Scintrex CG-5 value.

Table 3. Physical property measurements of rock samples collected in May 2007

Station	Rock type	Circular 91 geological unit ¹	Grain density (kg/m ³)	Saturated bulk density (kg/m ³)	Dry bulk density (kg/m ³)	Porosity (%)	Susceptibility (10 ⁻³ SI)
07s006	Carbonate	Owk	2780	2680	2630	5.4	0.03
07s024	Carbonate	DSO _h	2600	2470	2380	9.3	0.02
07s081	Carbonate	Ok	2800	2750	2720	3.2	0.03
07s089	Carbonate	Ow	2740	2650	2600	5.6	0.03
07s102	Carbonate	Ow	2800	2720	2670	4.9	0.02
07s139	Carbonate	Owk	2800	2780	2770	1.4	0.03
07s153	Granite	pCtr	2590	2530	2490	4.2	4.1
07s158	Carbonate	Owk	2810	2710	2660	5.9	0.02
07s161a	Mafic intrusive	pCti	3000	2990	2990	0.5	35
07s161b	Granite	pCti	2590	2560	2540	2.0	1.4
07s165	Carbonate	Ocm	2790	2720	2690	3.7	0.02

¹Circular 91 denotes Plate 1 of Fairchild and others (1990); Owk, Lower Ordovician West Spring Creek and Kindblade Formations (Arbuckle Group); DSO_h, Devonian, Silurian, and Ordovician Hunton Group; Ok, Lower Ordovician Kindblade Formation (Arbuckle Group); Ow, Lower Ordovician West Spring Creek Formation (Arbuckle Group); pCtr, Precambrian Troy Granite; pCti, Precambrian Tishomingo Granite; Ocm, Middle Ordovician Bromide, Tulip Creek, and McLish Formations (Simpson Group).

Table 4. Physical properties of rock samples grouped by stratigraphic unit

[Properties are averages followed by 1-standard deviation values in parentheses, except for the column containing the range of saturated bulk density. (NS) means not significant standard deviation value because too few measurements. Includes data from Table 2 of Scheirer and Hosford Scheirer (2006) and Table 3 of this study.]

Stratigraphic group	Age	Number of samples	Saturated bulk density (kg/m ³)	Saturated bulk density range (kg/m ³)	Porosity (%)	Susceptibility (10 ⁻³ SI)
Vanoss Group	Pennsylvanian	5	2440 (140)	2240-2590	7 (3)	0.02 (0.01)
Sycamore Ls./Weldon Ls./Woodford Shale	Mississippian/ Devonian	2	2520 (NS)	2450-2590	3 (NS)	0.01 (NS)
Hunton Group	Devonian/ Silurian/ Ordovician	2	2520 (NS)	2470-2570	7 (NS)	0.04 (NS)
Sylvan Shale/ Viola Group	Ordovician	2	2660 (NS)	2660-2660	0.7 (NS)	0.03 (NS)
Simpson Group	Ordovician	6	2480 (180)	2260-2660	5 (5)	0.03 (0.01)
Arbuckle Group	Ordovician/ Cambrian	17	2690 (60)	2550-2800	4 (2)	0.03 (0.01)
Basement	Precambrian	7	2670 (170)	2530-2990	1 (1)	11 (13)

References Cited

- Blakely, R.J., 1995, Potential theory in gravity and magnetic applications: Cambridge University Press, 441 p.
- Blakely, R.J., and Simpson, R.W., 1986, Approximating edges of source bodies from magnetic or gravity anomalies: *Geophysics*, v. 51, p. 1494-1498.
- Braile, L., 1989, Crustal structure of the continental interior, *in* Pakiser, L.C. and Mooney, W.D., Ed., *Geophysical Framework of the Continental United States: Geological Society of America Memoir 172*, p. 285-316.
- Cates, S. W., 1989, Fault distribution in the Sulphur, Oklahoma area based on gravity, magnetic and structural data: Norman, Okla., University of Oklahoma, M.S. Thesis, 106 p.
- Cederstrand, J.R., 1996, Digital geologic map of Ardmore-Sherman quadrangles, south-central Oklahoma: U.S. Geological Survey Open-File Report 96-370.
- Fairchild, R. W., R. L. Hanson, and R. E. Davis, 1990, Hydrology of the Arbuckle Mountains area, south-central Oklahoma: Norman, Okla., Oklahoma Geological Survey Circular 91, 112 p.
- Ham, W. E., 1969, Regional geology of the Arbuckle Mountains, Oklahoma: Norman, Okla., Oklahoma Geological Survey Guidebook 17, 52 p.
- Ham, W.E., McKinley, M.E., and others, 1954, Geologic map and sections of the Arbuckle Mountains, Oklahoma: Oklahoma Geological Survey Miscellaneous Map A-2, scale 1:72,000.
- Hanson, R. L., and S. W. Cates, 1994, Hydrogeology of the Chickasaw National Recreation Area, Murray County, Oklahoma: U.S. Geological Survey Water-Resources Investigations Report 94-4102, 86 p.
- Hart, D. L. J., 1974, Reconnaissance of the Water Resources of the Ardmore and Sherman Quadrangles, Southern Oklahoma: Oklahoma Geological Survey Hydrologic Atlas HA-3, scale 1:250,000.
- Hildenbrand, T.G., Briesacher, A., Flanagan, G., Hinze, W.J., Hittelman, A.M., Keller, G.R., Kucks, R.P., Plouff, D., Roest, W., Seeley, J., Smith, D.A., Webring, M., 2002, Rationale and operational plan to upgrade the U.S. Gravity Database: U.S. Geological Survey Open-File Report 02-463, 12p. [available on the World Wide Web at URL <http://geopubs.wr.usgs.gov/open-file/of02-463/>; data downloaded in October 2007 from URL <http://paces.geo.utep.edu/research/gravmag/gravmag.shtml>]
- Jablonski, H.M., 1974, World relative gravity reference network North America, Parts 1 and 2: U.S. Defense Mapping Agency Aerospace Center Reference Publication no. 25, originally published 1970, revised 1974, with supplement of IGSN 71 gravity datum values, 1261 p.
- Johnson, G.R., and Olhoef, G.R., 1984, Density of rocks and minerals, *in* Carmichael, R.S., ed., *CRC Handbook of Physical Properties of Rocks*, Vol. 3: Boca Raton, Fla., CRC Press, Inc., p. 1-38.
- Johnson, K.S., 1990, Geologic map and sections of the Arbuckle Mountains, Oklahoma, revision of Ham, W.E., McKinley, M.E., and others, 1954: Norman, Okla., Oklahoma Geological Survey Circular 91, scale 1:100,000.
- Oklahoma Water Resources Board, 2003, The Arbuckle-Simpson hydrology study— Management and protection of an Oklahoma water resource: Oklahoma Water Resources Board Fact Sheet, 4 p.
- Plouff, D., 1977, Preliminary documentation for a FORTRAN program to compute gravity terrain corrections based on topography digitized on a geographic grid: U.S. Geological Survey Open-File Report 77-535, 45 p.
- Scheirer, D.S., and Hosford Scheirer, A., 2006, Gravity investigations of the Chickasaw National Recreation Area, south-central Oklahoma: U.S. Geological Survey Open-File Report 2006-1083, 40 p. [available on the World Wide Web at URL <http://pubs.usgs.gov/of/2006/1083/>]
- Simpson, R.W., Jachens, R.C., Blakely, R.J., and Saltus, R.W., 1986, A new isostatic residual gravity map of the conterminous United States with a discussion on the significance of isostatic residual anomalies: *Journal of Geophysical Research*, v. 91, p. 8348-8372.
- Smith, B.D., Smith, D.V., Blome C.D., and Hill, P., in review, Helicopter electromagnetic and magnetic geophysical survey data, Hunton Anticline, south-central Oklahoma: U.S. Geological Survey Open-File Report in review.
- Sweeney, R.E., and Hill, P.L., 2005, Nebraska, Kansas, and Oklahoma aeromagnetic and gravity maps and data: A web site for distribution of data: U.S. Geological Survey Data Series 138. [available on the World Wide Web at URL <http://pubs.usgs.gov/ds/2005/138/>]
- Talwani, M., Worzek, J.L., and Landisman, M., 1959, Rapid gravity computations for two-dimensional bodies with application to the Mendocino submarine fracture zone: *Journal of Geophysical Research*, v. 64, p. 49-59.

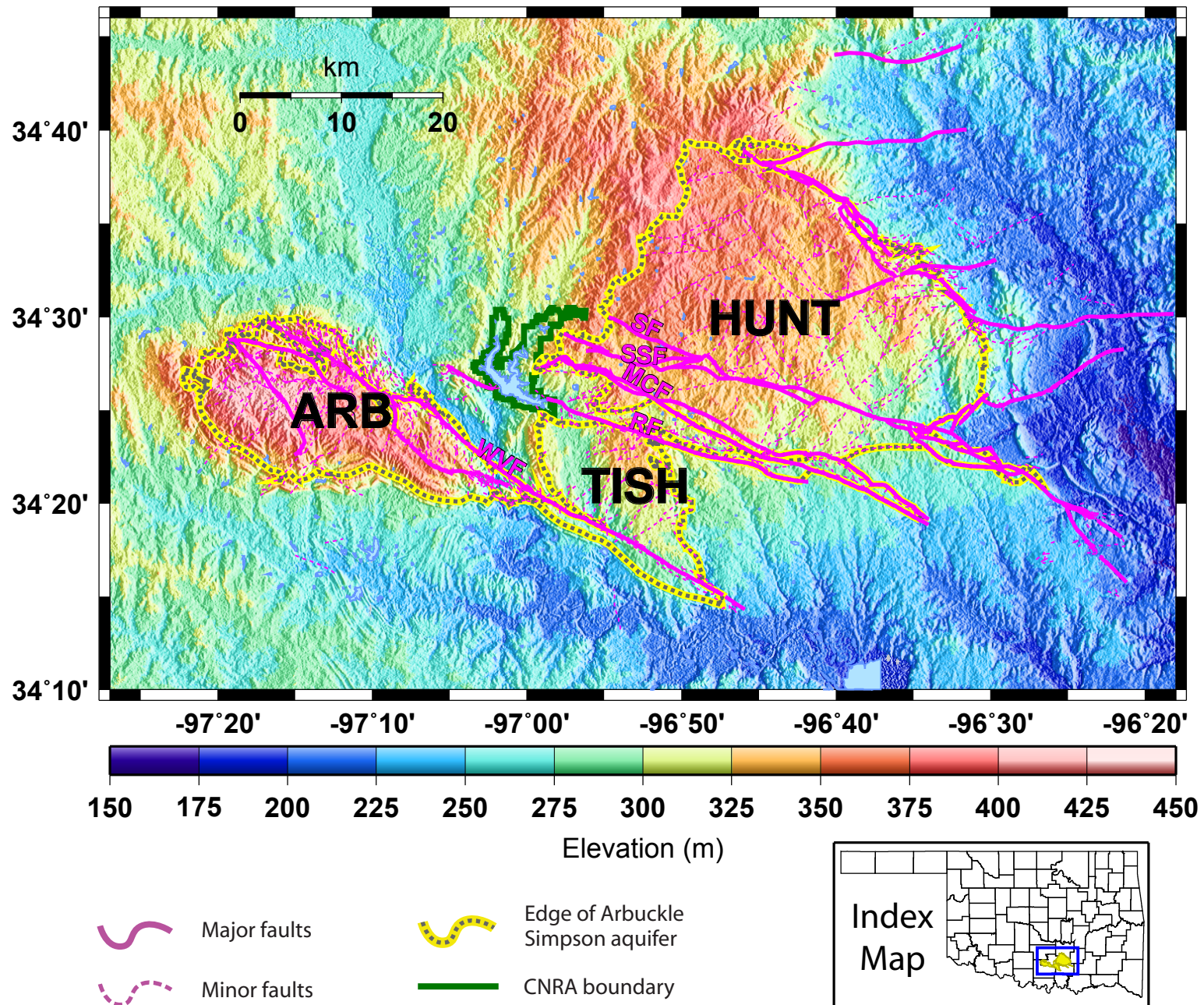


Figure 1. 1a) Topographic map of the Arbuckle Uplift. The Arbuckle, Tishomingo, and Hunton Anticlines are designated by ARB, TISH, and HUNT, respectively. SF=Sulphur Fault; SSF=South Sulphur Fault; MCF=Mill Creek Fault; RF=Reagan Fault; WVF=Washita Valley Fault. Index map of Arbuckle-Simpson aquifer outcrop (yellow) in south-central Oklahoma; map area is denoted by blue rectangle superimposed on Oklahoma county outlines.

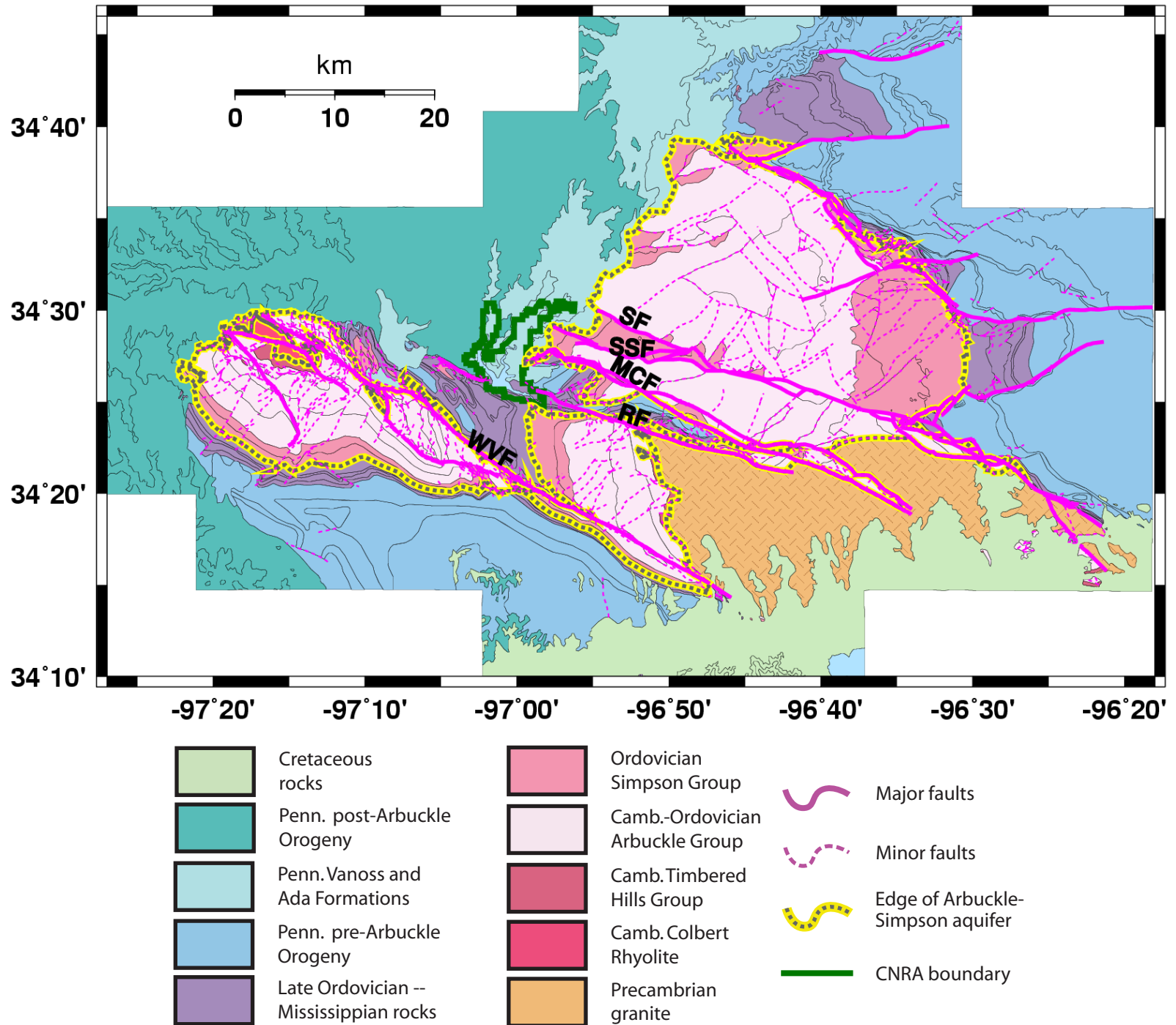


Figure 1. 1b) Bedrock geology and faults of the Arbuckle Uplift, based on mapping of Ham and others (1954), transcribed by Hart (1974), and digitized by Cederstrand (1996) with edits by the Oklahoma Water Resources Board (2004, personal commun.).

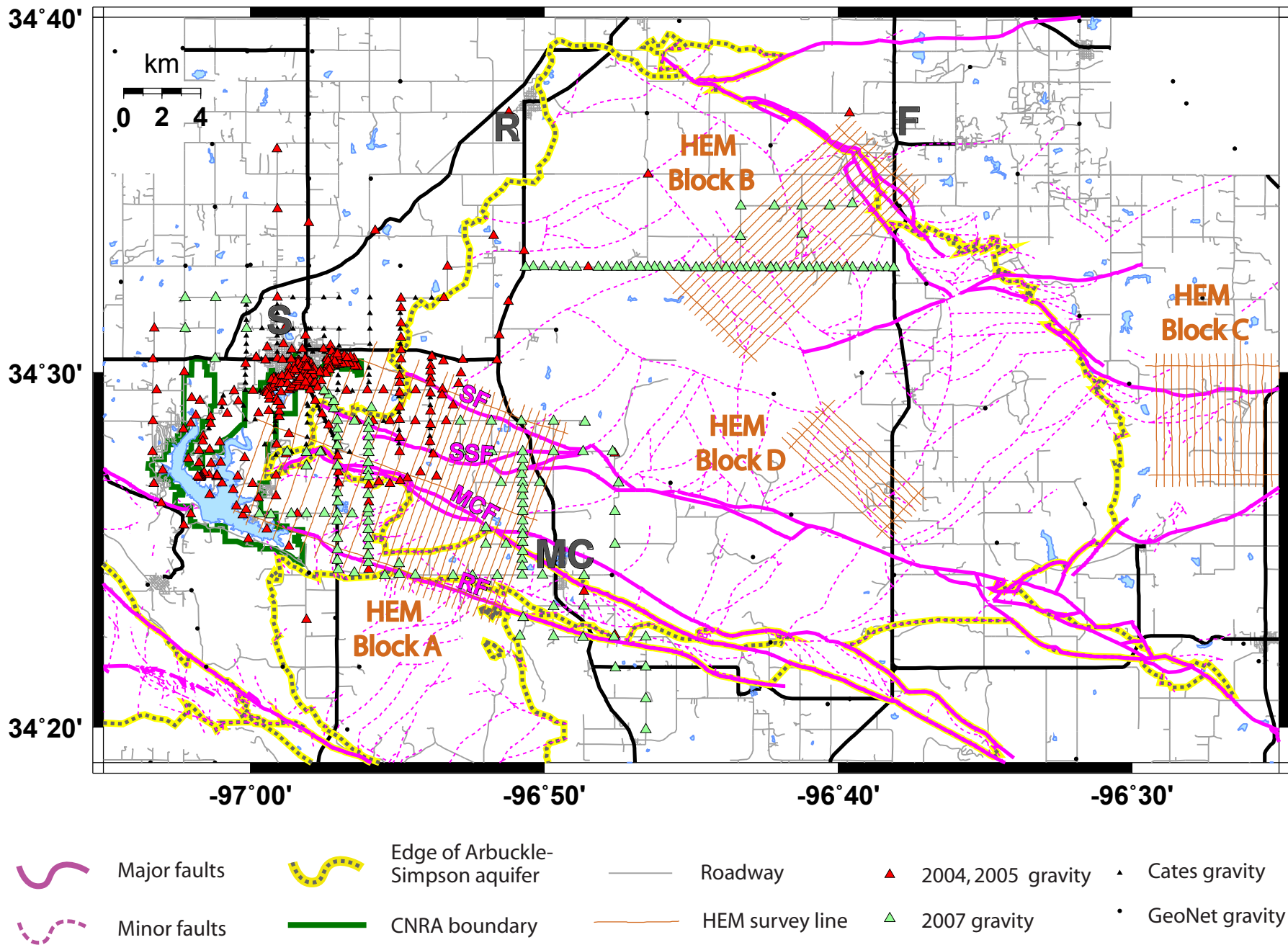


Figure 2. Map of gravity stations collected in May 2007 (green triangles). Gravity stations collected by the USGS in 2004 and 2005 (Scheirer and Hosford Scheirer, 2006) are shown as red triangles; stations collected by Cates (1989) are black triangles; regional stations from the GeoNet database (Hildenbrand and others, 2002) are black circles. Brown lines show flight-lines of the March 2007 helicopter electromagnetic (HEM) and aeromagnetic survey. Town abbreviations: S=Sulphur, R=Roff, MC=Mill Creek, F=Fittstown. Fault abbreviations: SF=Sulphur Fault, SSF=South Sulphur Fault, MCF=Mill Creek Fault, RF=Reagan Fault.

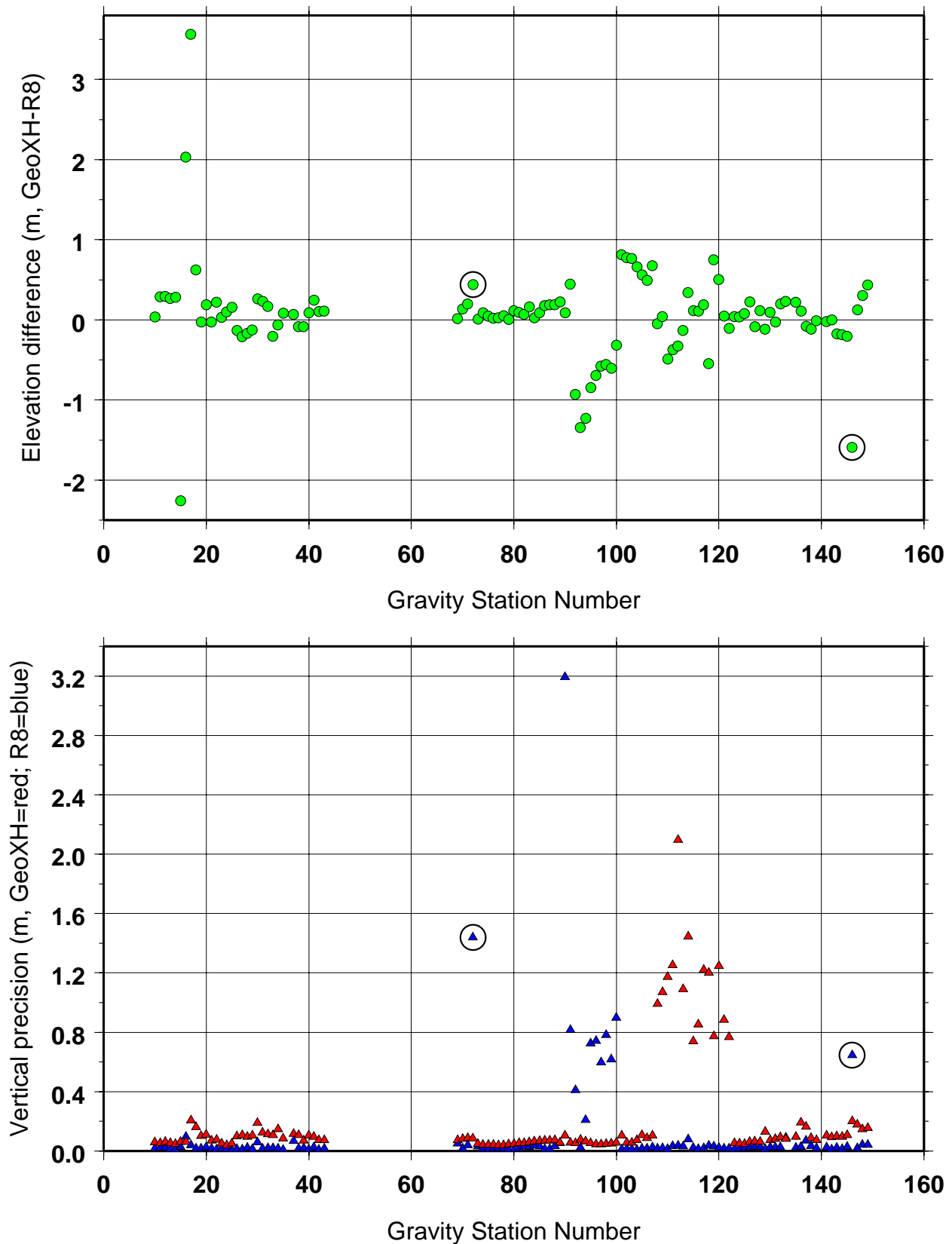


Figure 3. (top panel) Difference between gravity station elevations determined by the Trimble GeoXH and Trimble R8 GPS units. Circled symbols denote the two instances of Trimble R8 FLOAT, as opposed to FIXED, solutions. (bottom panel) Precisions for GeoXH (red symbols, calculated by Trimble Pathfinder Office software) and R8 (blue symbols, calculated by Trimble Geomatics Office software) GPS solutions. The only GeoXH precisions >0.7 m are associated with the gravity stations of 2007May14. R8 precisions >0.2m occurred with FLOAT solutions (circled) and during a 1.5 hour window in the early afternoon of 2007May12. Note that the calculated vertical precisions of gravity station locations, generally <0.2 m in bottom panel, sometimes exceed the corresponding elevation difference in the top panel.



Figure 4. Scintrex CG-5 gravity meter prepared for taking a reading at a gravity station. Of the two visible GPS antennas on the roof, the Trimble R8 receiver is toward the rear and the Trimble GeoXH Zephyr antenna is toward the front of the vehicle.

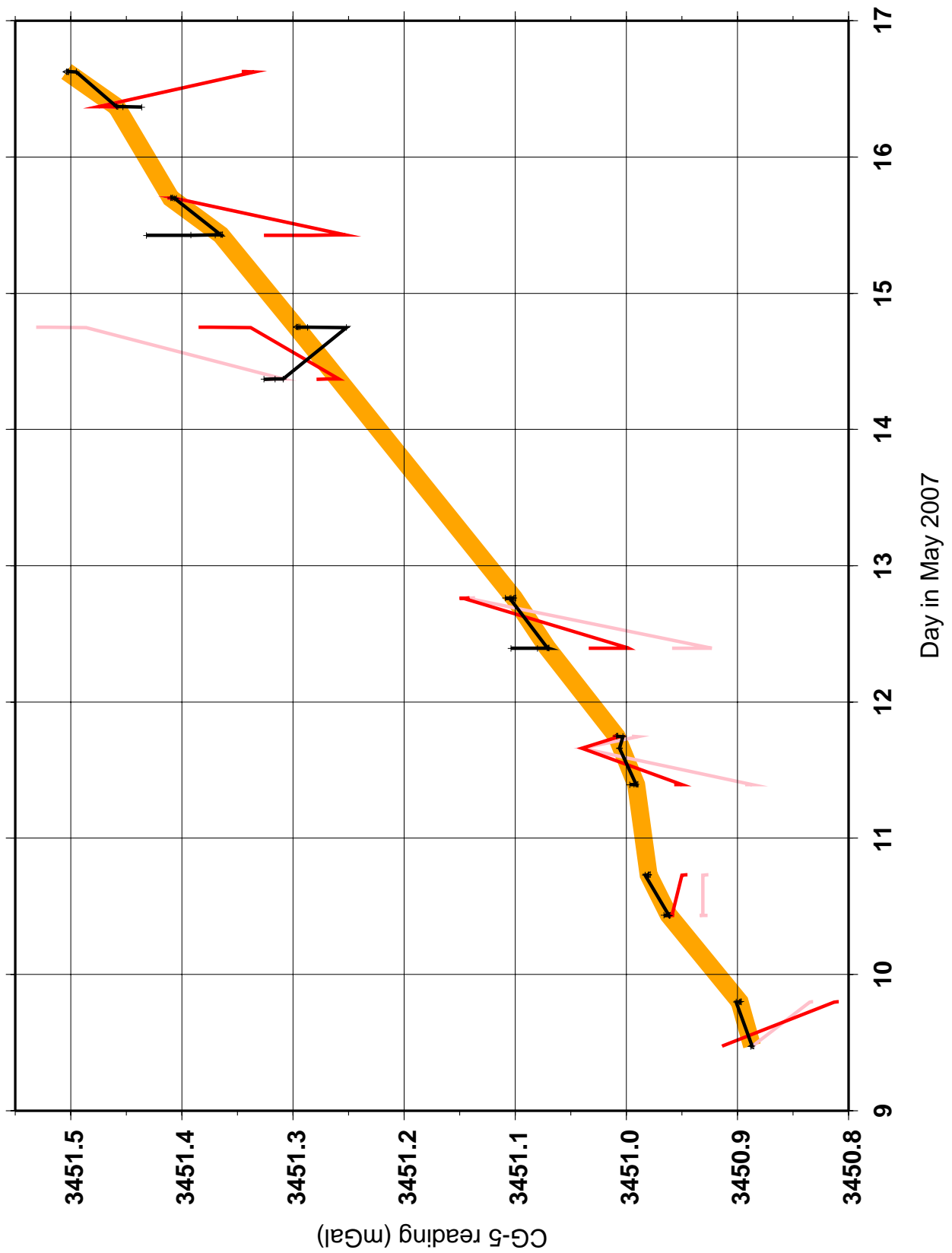


Figure 5. Drift curve (orange) for Scintrex CG-5 gravity meter. Black lines link tide-corrected readings for all of the PVENDOME readings; red lines indicate reading values not corrected for tides; pink lines indicate readings with wrong tide corrections that were observed in the field.

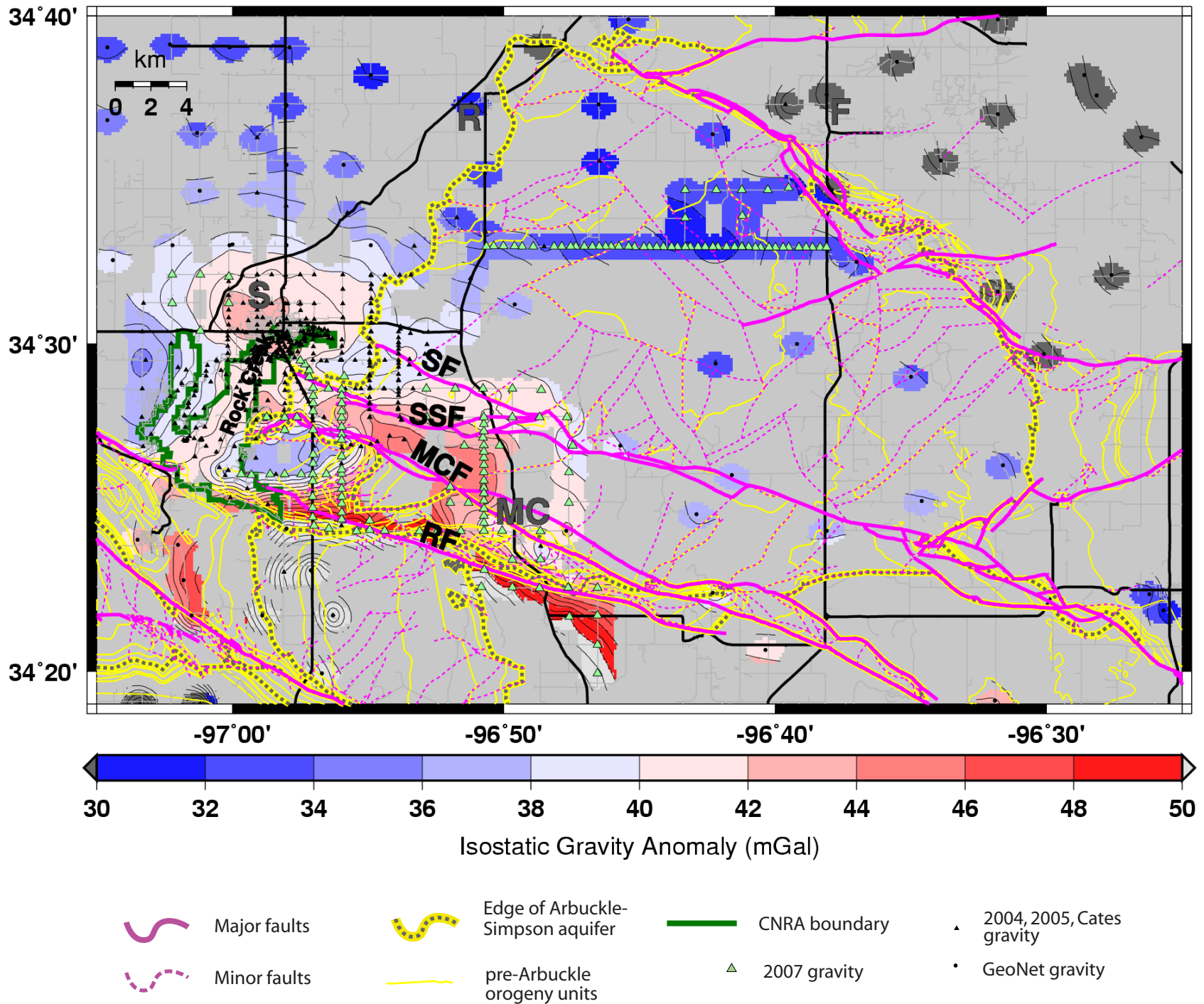
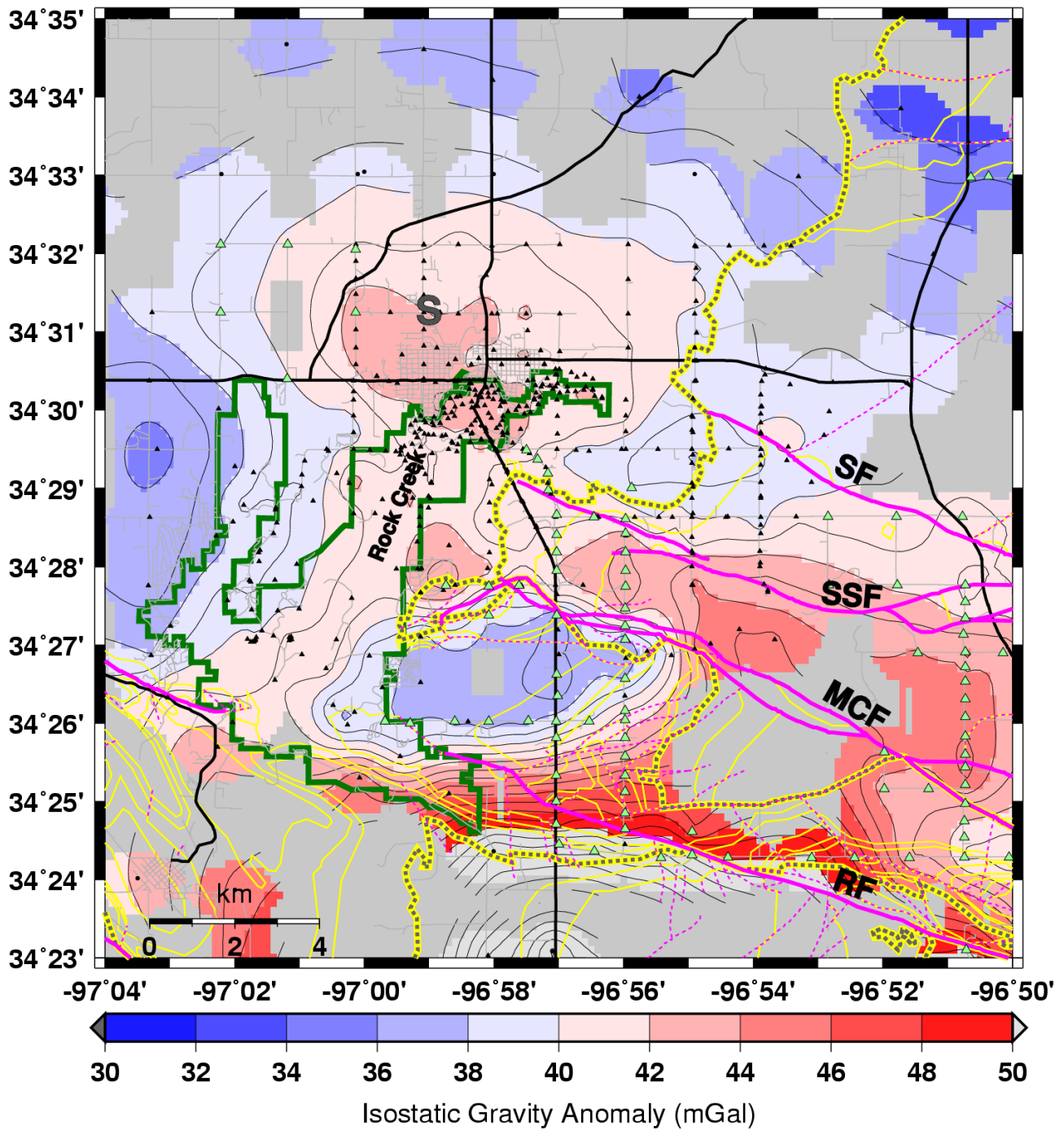


Figure 6a. Isostatic gravity map of Hunton Anticline region. Contour interval is 1 mGal. Gravity stations collected in May 2007 are indicated by green triangles; prior gravity stations indicated by black symbols.



- | | | | |
|---|----------------------------------|---|---------------------------|
|  | Major faults |  | CNRA boundary |
|  | Minor faults |  | 2004, 2005, Cates gravity |
|  | Edge of Arbuckle-Simpson aquifer |  | 2007 gravity |
|  | pre-Arbuckle orogeny units |  | GeoNet gravity |

Figure 6b. Isostatic gravity map of Chickasaw National Recreation Area (green line) and area immediately to east. Contour interval is 1 mGal. Gravity stations collected in May 2007 are indicated by green triangles; prior gravity stations indicated by black symbols.

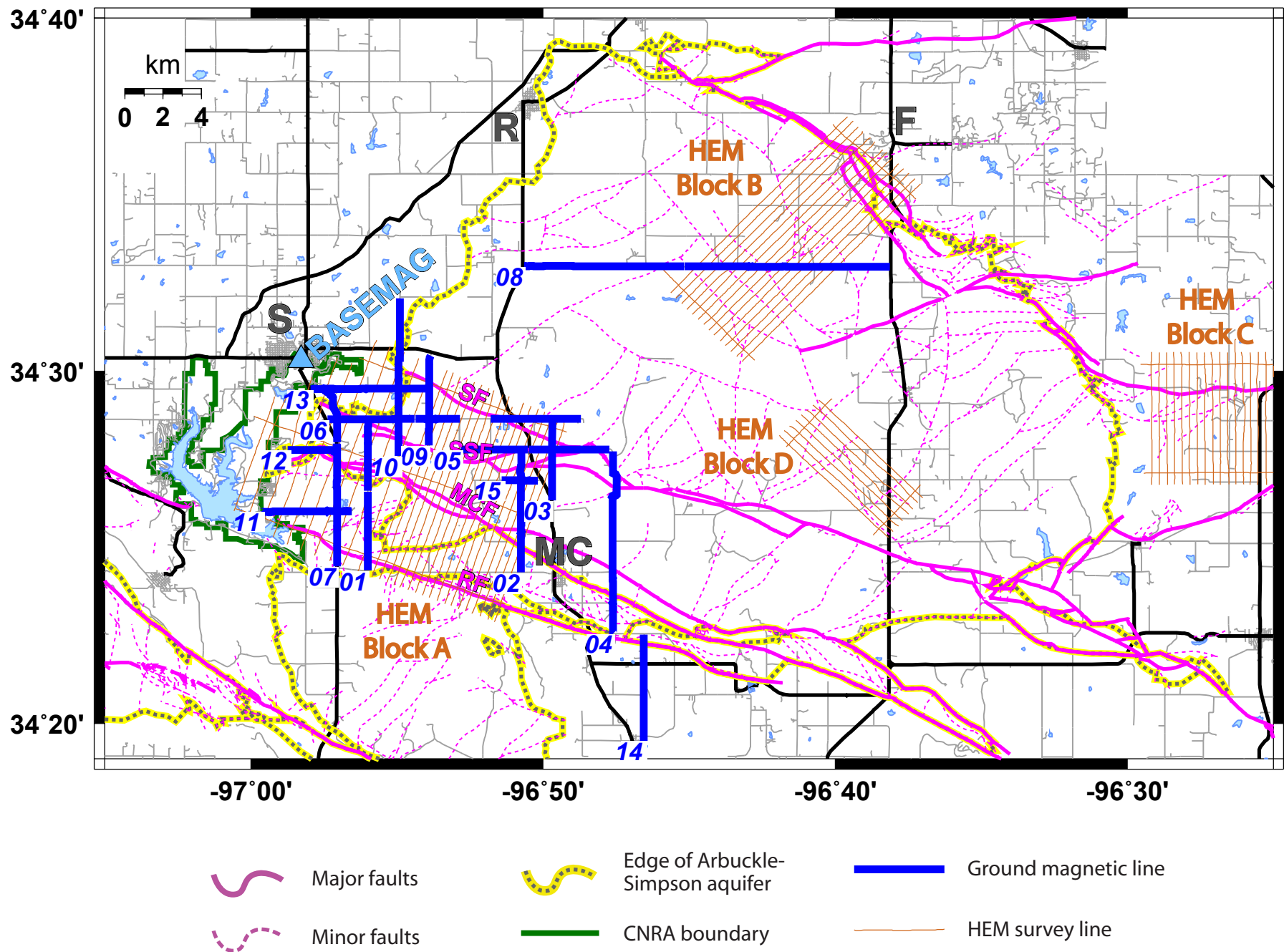


Figure 7. Map of magnetic lines (blue) collected in May 2007. The magnetic base location is designated BASEMAG. Other plot elements are the same as in Figure 2.



Figure 8. Geometrics G-856 proton precession magnetic base station at a temporary site near BOSTICK on 2007May08. The controller and battery are not shown in this photograph. At this site, base data were noisier than data collected on subsequent days at a site near Vendome Well, CNRA.

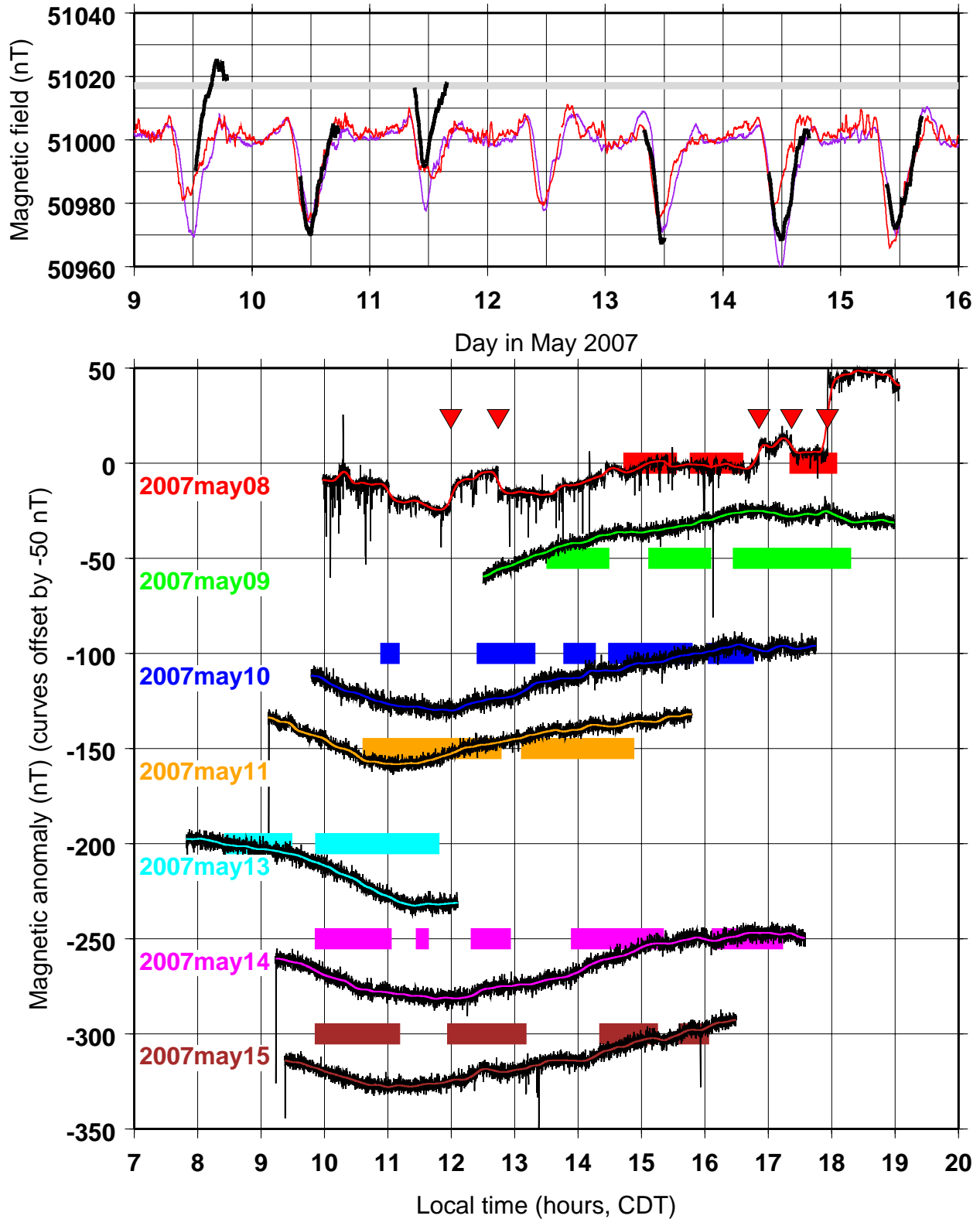


Figure 9a. (Top panel) Total field variation, black line, at the magnetic base station near Vendome Well, CNRA. Horizontal gray line indicates the IGRF2005 predicted value of the total field at this location. Purple line is the total field variability at magnetic observatory BOU (Boulder, CO); red line is BSL (Bay St. Louis, MS); observatory curves have been time-adjusted for site longitude differences. (Bottom panel) Total field variation at the base station during the 7 days when we conducted walking surveys. Anomalies are offset by -50 nT on successive days for clarity. The site of the magnetic base station on 2007May08 was influenced by vehicles either parking in or leaving neighboring driveways at times indicated by red triangles. Magnetic base data were collected on subsequent days at a site near Vendome Well, which had minimal anthropogenic influence. Black lines indicate the raw magnetic values every 5 seconds; colored lines are filtered anomalies. Horizontal bars indicate times of walking survey lines.

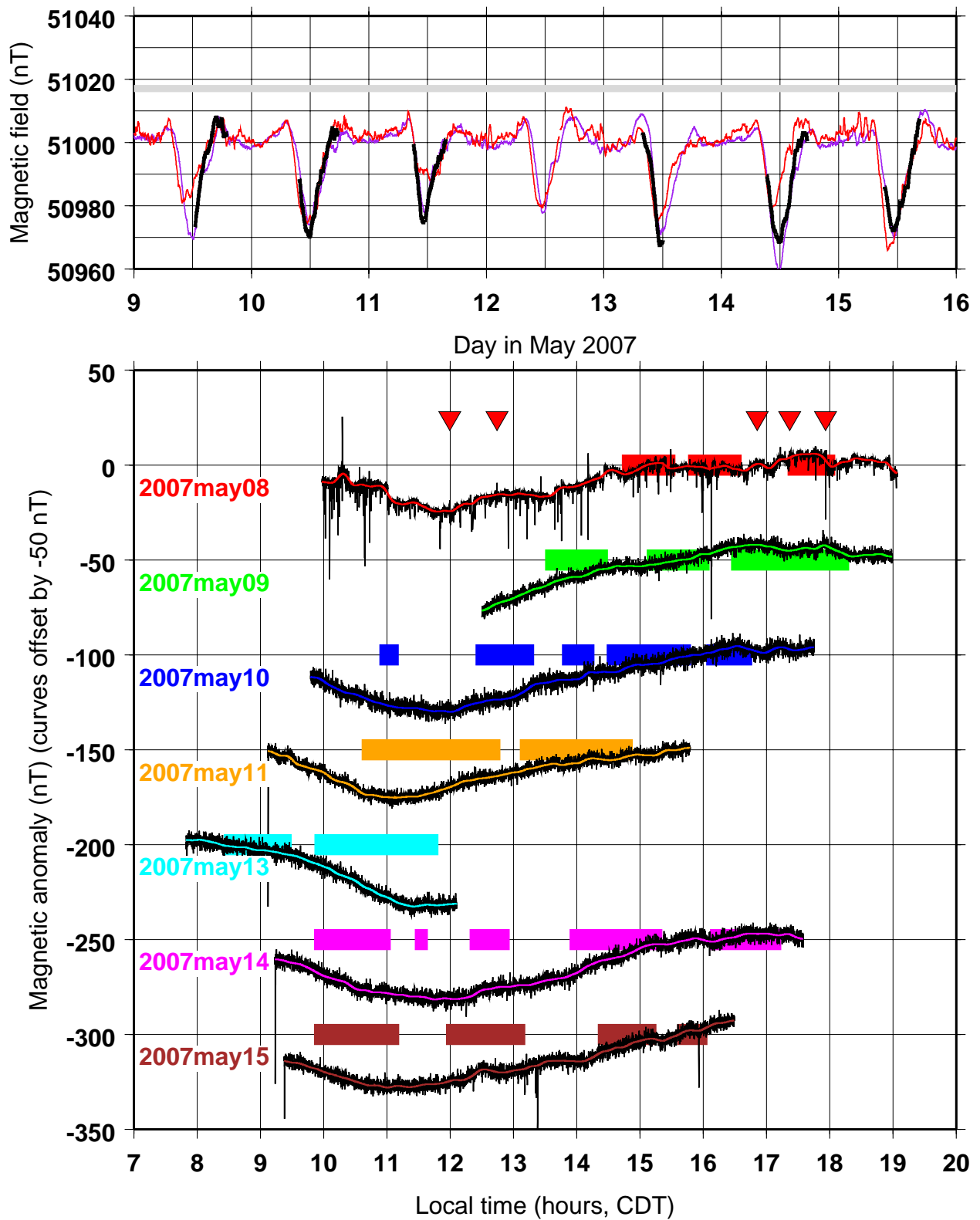


Figure 9b. Total field variation, corrected for near-site variations on 2007May08 and for constant shifts on 2007May09 and 2007May11. Same plot elements as in Figure 9a.



Figure 10. (top) Essam About walking with the Geometrics G-858 cesium magnetometer backpack system. Two cesium magnetometer sensors were deployed on the tall pole 2007May08, above; on other days, we deployed only the upper sensor to conserve battery power. A non-magnetic Trimble Ag-GPS132 antenna is mounted at the top of the short pole, and the battery and GPS receiver are at the base of the backpack. (bottom) Joseph Zume walks with the backpack magnetometer system in a magnetically noisy environment. Bridges and power lines produce large magnetic signals that need to be removed before geological analysis.

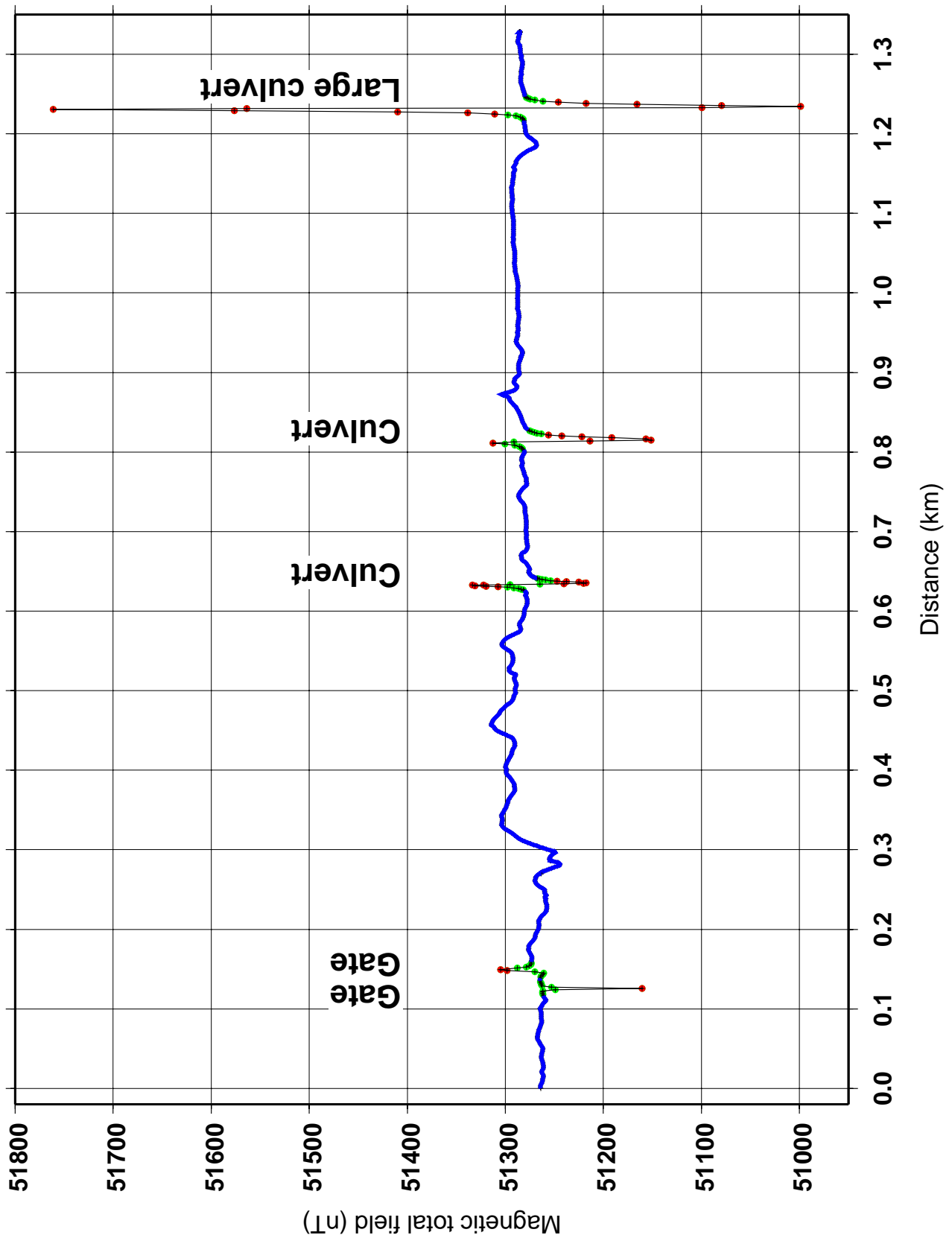


Figure 11. Magnetic field variability of raw 1-second data from a ~1.3 km span, collected during 20 minutes near the western end of the profile along the seismic line road (2007May11). Short-wavelength anomalies arise from metallic gates along the roadway near a ranch-house and from culverts crossing beneath the roadbed. Red circles indicate observations rejected by the time-series filter cascade because they differ greatly from regional values; green circles indicate points rejected because they are in close proximity to observations with great differences.

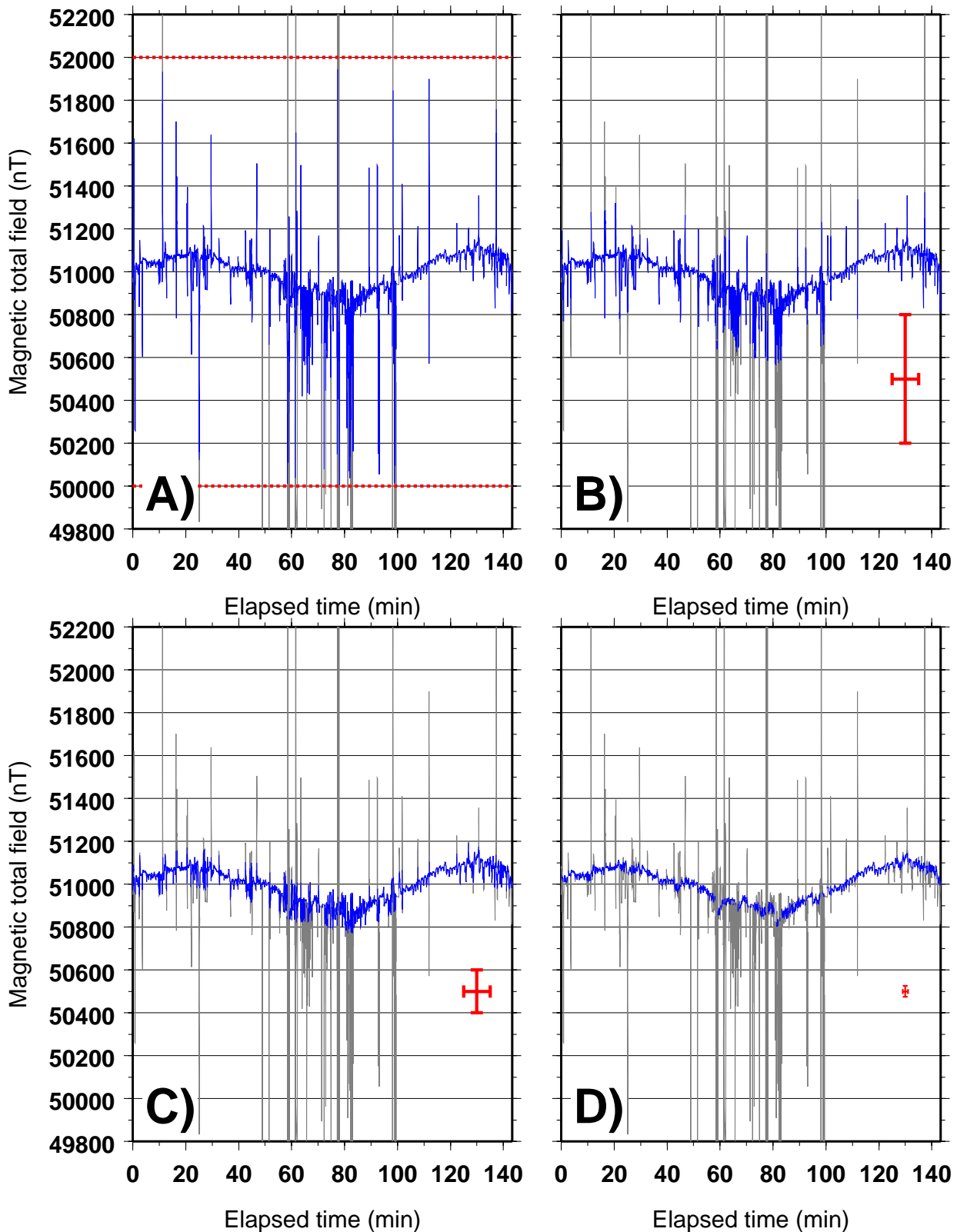


Figure 12. Panels illustrating the effects of the cascade of time-series filters on magnetic data collected on 2007May08, a ~2.3 hour time-span that is representative of the signal/noise character of the entire data set. In all cases, raw magnetic data are shown in black. A) Magnetic values were voided when >1000 nT (red dashed lines) from an average IGRF2005 value for the study area and when collected at times when we were stationary. B) Additional magnetic values were voided when they differed by >300 nT from the median value of centered, 10-minute (600-sec) time-window of observations. The red cross illustrates the time and magnetic anomaly spans of this filter. C) Additional magnetic values were voided when they differed by >100 nT from the median value of centered, 10-minute time-windows (red cross). D) Additional magnetic values were voided when they differed by >25 nT from the median value of centered, 2-minute time-windows (red cross).

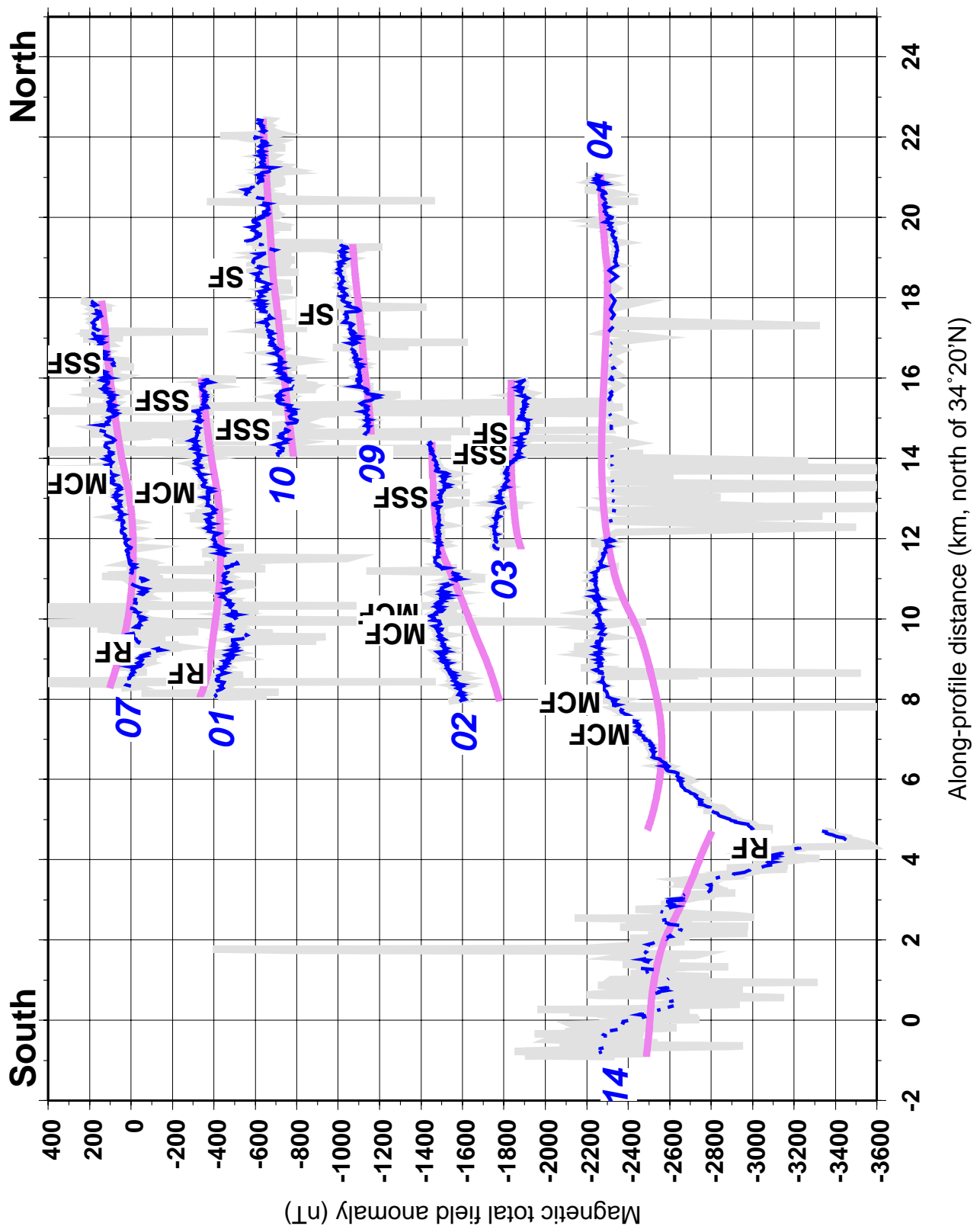


Figure 13. a) Magnetic anomalies of the 8 south-to-north magnetic profiles; see Figure 7 for locations. The profiles are arranged from west to east and are offset successively by 300 nT for clarity. Blue line corresponds to filtered ground magnetic anomaly; gray line is unfiltered ground magnetic anomaly, and purple line is gridded aeromagnetic anomaly from Sweeney and Hill (2005). Where the blue line is absent, especially in lines 14 and 04, the raw magnetic anomaly was too noisy to pass a value through the filter cascade. Locations of fault trace crossings are labeled: RF=Reagan Fault; MCF=Mill Creek Fault; SSF=South Sulphur Fault; SF=Sulphur Fault.

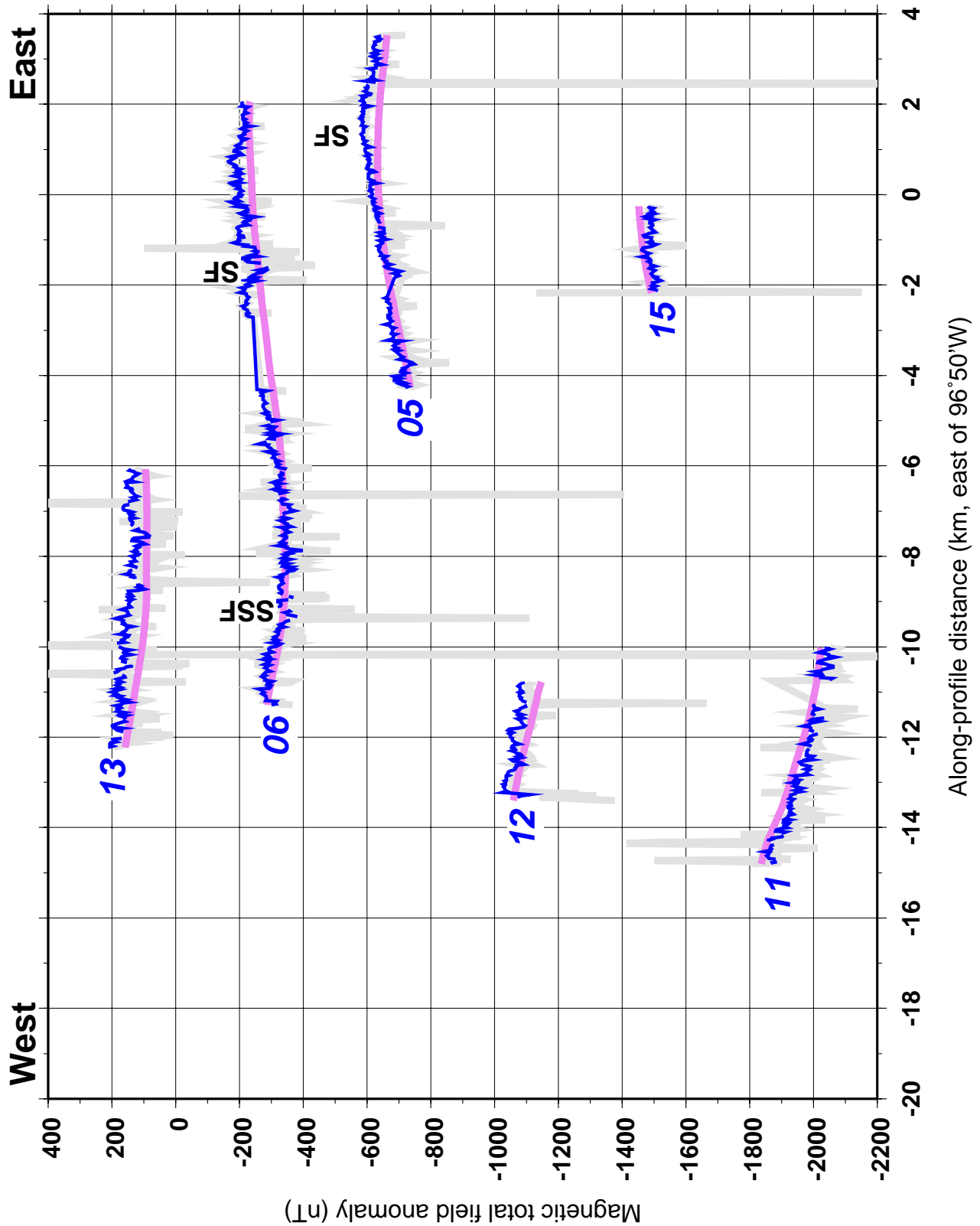


Figure 13. (ctd.) b) Magnetic anomalies of the 6 west-to-east magnetic profiles; see Figure 7 for locations. The profiles are arranged from north to south and are offset successively by 300 nT for clarity. Blue line corresponds to filtered ground magnetic anomaly; gray line is unfiltered ground magnetic anomaly, and purple line is gridded aeromagnetic anomaly from Sweeney and Hill (2005). Locations of fault trace crossings are labeled: SSF=South Sulphur Fault; SF=Sulphur Fault. Fault crossings are more oblique for these lines than for the south-to-north lines (Figure 13a).

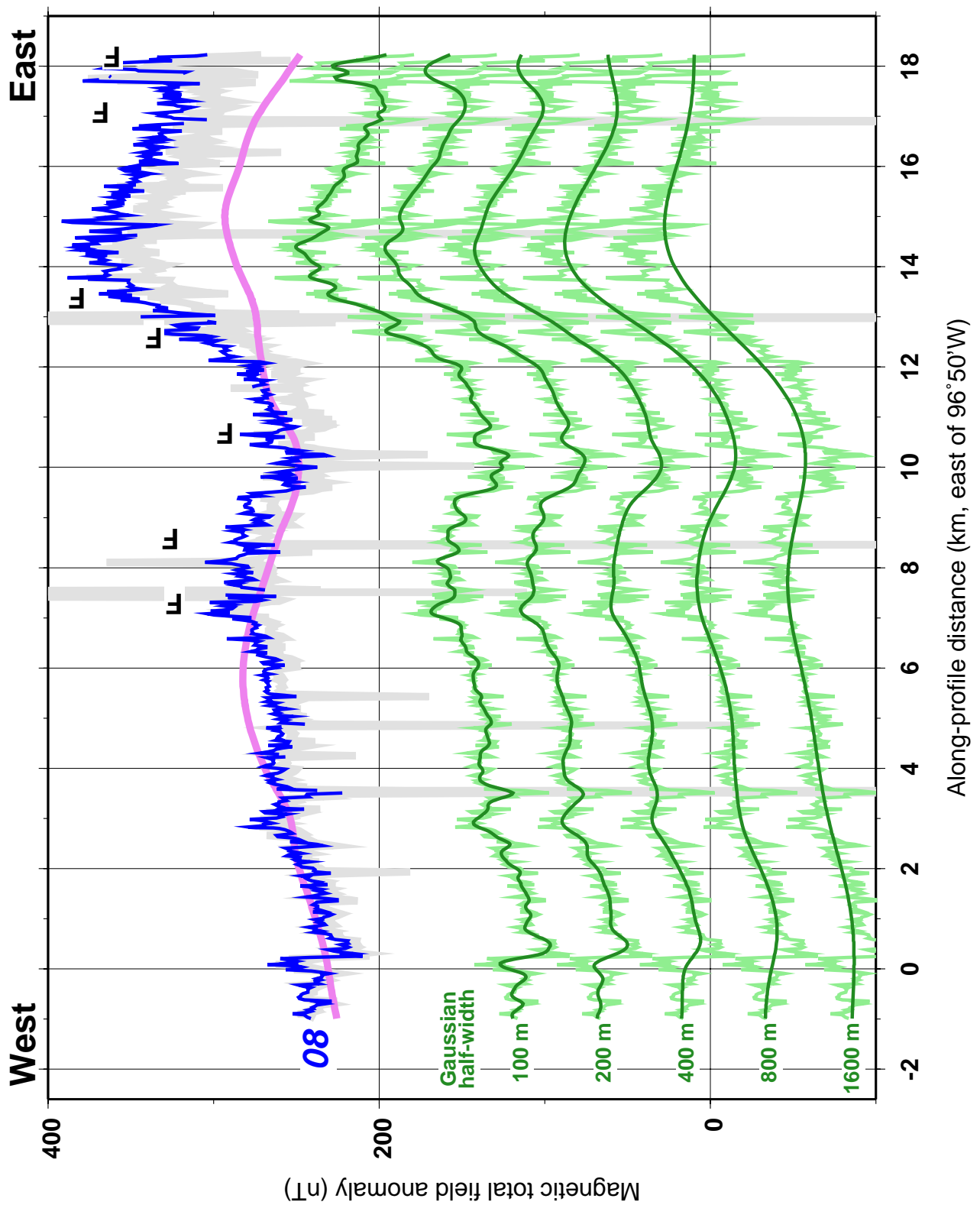


Figure 13. (ctd.) c) Magnetic anomalies of the west-to-east profile along the seismic line; see Figure 7 for location. Blue line corresponds to filtered ground magnetic anomaly; gray line is unfiltered ground magnetic anomaly, and purple line is gridded aeromagnetic anomaly from Sweeney and Hill (2005). Offset dark green lines illustrate different smoothing operations on the filtered ground magnetic anomaly (light green); from top to bottom, convolutions with Gaussian functions having standard deviation widths of 100 m, 200 m, 400 m, 800 m, 1600 m, respectively. Locations of minor fault crossings are marked with F.

Appendix: Gravity base stations established by the U.S. Geological Survey near Sulphur, Oklahoma

Data sheets for two of the gravity base stations established in Chickasaw National Recreation Area, south-central Oklahoma, are provided below.

Gravity Base VENDOME

General location: Adjacent to Vendome Well, Chickasaw National Recreation Area, Sulphur, Oklahoma

Established by: Daniel Scheirer (US Geological Survey) on 2004Jun12

Position (NAD27) **34° 30.348'N** **96° 58.378'W**

Elevation (NGVD29) **288.4 m**

Position (NAD83) **34° 30.353'N** **96° 58.396'W**

Elevation (NAVD29) **288.5 m**

Location is based on Trimble GeoXT GPS receiver data collected on 2004Jun12.

Gravity value (IGSN71): 979,648.02 mGal

Based on double-loop to World Relative Gravity Reference Network base station COALGATE on 2004Jun12 with LaCoste-Romberg gravimeter G17C.

Detailed description: Gravity meter is placed near drinking-fountain, at northern edge of the outlet pool of Vendome Well, centered on the strip of concrete adjacent to the wall. Center of base plate is 25 cm from outer edge of the outlet pool wall.

Reference: Scheirer, D.S., and Hosford Scheirer, A., 2006, Gravity investigations of the Chickasaw National Recreation Area, south-central Oklahoma: U.S. Geological Survey Open-File Report 2006-1083, 40p.

Photographs of outlet pool of Vendome Well showing the location of gravity base VENDOME. Photographs were taken in June 2004.



Gravity Base PVENDOME

General location: Western end of parking lot for Vendome Well, Chickasaw National Recreation Area, Sulphur, Oklahoma

Established by: Daniel Scheirer (US Geological Survey) on 2005Apr24

Position (NAD27) **34° 30.346'N 96° 58.353'W**

Elevation (NGVD29) **287.8 m**

Position (NAD83) **34° 30.351'N 96° 58.371'W**

Elevation (NAVD29) **287.9 m**

Location is based on Trimble GeoXT GPS receiver data collected on 2005May02.

Gravity value (IGSN71): 979,648.08 mGal

Based on multiple loops to gravity base VENDOME in 2004 June, 2005 April, and 2007 May with LaCoste-Romberg gravimeters G17C, G425, G8N, and a Scintrex CG5 gravimeter.

Detailed description: Gravity meter base plate is centered on largest clast in the asphalt pavement adjacent to large tree at western edge of parking lot for Vendome Well. The tree is immediately south of where the well outflow goes beneath parking lot.

Reference: Scheirer, D.S., and Hosford Scheirer, A., 2006, Gravity investigations of the Chickasaw National Recreation Area, south-central Oklahoma: U.S. Geological Survey Open-File Report 2006-1083, 40p.

Modified IGSN71 value for PVENDOME described in: Scheirer, D.S., and Aboud, E., 2007, Preliminary gravity and ground magnetic data in the Arbuckle Uplift near Sulphur, Oklahoma: U.S. Geological Survey Open-File Report 2008-1003, 34 p.

Photographs showing the location of gravity base PVENDOME. Photo on left is view towards the WNW, and base location is surrounded by pens. Photographs were taken in May 2007.

